

Structured barycentric forms for interpolation-based data-driven reduced modeling of second-order systems

Ion Victor Gosea* Serkan Gugercin[†] Steffen W. R. Werner[‡]

* *Max Planck Institute for Dynamics of Complex Technical Systems, Sandtorstr. 1, 39106 Magdeburg, Germany.*

Email: gosea@mpi-magdeburg.mpg.de, ORCID: [0000-0003-3580-4116](https://orcid.org/0000-0003-3580-4116)

[†] *Department of Mathematics and Division of Computational Modeling and Data Analytics, Academy of Data Science, Virginia Tech, Blacksburg, VA 24061, USA.*

Email: gugercin@vt.edu, ORCID: [0000-0003-4564-5999](https://orcid.org/0000-0003-4564-5999)

[‡] *Courant Institute of Mathematical Sciences, New York University, New York, NY 10012, USA.*

Email: steffen.werner@nyu.edu, ORCID: [0000-0003-1667-4862](https://orcid.org/0000-0003-1667-4862)

Abstract: An essential tool in data-driven modeling of dynamical systems from frequency response measurements is the barycentric form of the underlying rational transfer function. In this work, we propose structured barycentric forms for modeling dynamical systems with second-order time derivatives using their frequency domain input-output data. By imposing a set of interpolation conditions, the systems' transfer functions are rewritten in different barycentric forms using different parametrizations. Loewner-like algorithms are developed for the explicit computation of second-order systems from data based on the developed barycentric forms. Numerical experiments show the performance of these new structured data driven modeling methods compared to other interpolation-based data-driven modeling techniques from the literature.

Keywords: data-driven modeling, second-order systems, reduced-order modeling, rational functions, barycentric forms, interpolation

Mathematics subject classification: 41A20, 65D05, 93B15, 93C05, 93C80

Novelty statement: We develop new structured barycentric forms for the transfer functions of second-order systems that allow structured data-driven modeling from frequency domain input-output data. For the explicit computation of second-order systems from data, interpolation-based Loewner-like algorithms are proposed.

1 Introduction

Data-driven reduced-order modeling, i.e., the construction of models describing the underlying dynamics of unknown systems from measurements, has become an increasingly preminent discipline. It is an essential tool in situations when explicit models in the form

of state space formulations are not available, yet abundant input/output data are, motivating the need for data-driven modeling. Depending on the underlying physics, dynamical systems can inherit differential structures leading to specific physical interpretations. In this work, we concentrate on systems that are described by differential equations with second-order time derivatives of the form

$$\begin{aligned} M\ddot{\mathbf{x}}(t) + D\dot{\mathbf{x}}(t) + K\mathbf{x}(t) &= \mathbf{b}u(t), \\ y(t) &= \mathbf{c}^\top \mathbf{x}(t), \end{aligned} \quad (1)$$

with $M, D, K \in \mathbb{R}^{n \times n}$ and $\mathbf{b}, \mathbf{c} \in \mathbb{R}^n$. Systems like (1) typically appear in the modeling of mechanical, electrical, and related structures [1, 11, 21, 23]. In the frequency domain (also known as the Laplace domain), the input-to-output behavior of (1) is equivalently given by the corresponding *transfer function*

$$H(s) = \mathbf{c}^\top (s^2 M + sD + K)^{-1} \mathbf{b}, \quad (2)$$

which is a degree- $2n$ rational functions in s , where n is the state-space dimension of (1).

In recent years, several methods have been developed for learning reduced-order state-space representations of dynamical systems from given data. However, most of these approaches consider the classical, *unstructured* case of first-order systems of the form

$$\begin{aligned} E\dot{\mathbf{x}}(t) &= A\mathbf{x}(t) + \mathbf{b}u(t), \\ y(t) &= \mathbf{c}^\top \mathbf{x}(t), \end{aligned} \quad (3)$$

where $E, A \in \mathbb{R}^{n \times n}$ and $\mathbf{b}, \mathbf{c} \in \mathbb{R}^n$, with the transfer function

$$H(s) = \mathbf{c}^\top (sE - A)^{-1} \mathbf{b}. \quad (4)$$

Examples for such methods are the subspace identification framework [18–20], dynamic mode decomposition [35, 40], operator inference [27, 29, 33], the Loewner framework [22, 28], rational least-squares methods such as vector fitting [14, 17] or RKFIT [8], or the transfer-function based \mathcal{H}_2 -optimal model reduction [7]. See also [12] for a more general introduction to this topic. The importance of preserving internal system structures in the computation of reduced-order approximations of dynamical systems for the case of second-order systems (1) has been observed in [34, 42], which allows in particular the reinterpretation of system quantities, the preservation of structure-inherent properties and provides cheap-to-evaluate models with high accuracy. However, only a few data-driven approaches have been recently extended to (1) such as the Loewner framework [30, 36] and operator inference [15, 37].

In this work, we concentrate on the case in which input-output measurements are available in the frequency domain, i.e., evaluations of the system’s transfer function (2). For this type of data, the goal in data-driven reduced-order modeling is the construction of low-order rational functions $\widehat{H}(s)$ that approximate the given data well in an appropriate measure. These rational functions can be interpreted as transfer functions corresponding to dynamical systems. Typically, it is not possible to extract additional differential structures from general rational functions. For example, even though one can always convert the structured transfer function in (2) to an unstructured rational function in (4), the reverse direction is not guaranteed. Most methods for learning transfer functions from frequency domain data have been mainly developed for the unstructured case (3). In particular, such methods include the barycentric Loewner framework [2], the vector fitting algorithm [14, 17] and the AAA algorithm [24]. The backbone of these methods is

the barycentric form of rational functions, which allows for computationally efficient constructions of rational interpolants and least-squares fits [9]. Enforcing structures in the barycentric form allows the design of structured data-driven modeling algorithms. In [44], this idea led to the extension of the vector fitting algorithm towards mechanical systems with modal damping structure.

In this paper, we develop new structured barycentric forms associated with the transfer functions of second-order systems (2). By enforcing interpolation conditions, we show that the system matrices in (1) satisfy certain equality constraints. Using different parametrizations of the matrices in (1), we derive corresponding structured barycentric forms that allow an easy construction of the system matrices (1) and enforce interpolation by construction. We are using free parameters in the barycentric forms that are not bound in the derivation, in order to design several Loewner-like algorithms, allowing the direct construction of second-order systems from given frequency domain data with interpolating transfer functions. We also present several strategies that allow the choice of free parameters in the structured barycentric forms to enforce additional properties in the constructed system matrices such as positive definiteness. Numerical examples are used to verify the developed theory and algorithms based on these barycentric forms.

The rest of the paper is organized as follows: In Section 2, we include mathematical preliminaries, needed for the theoretical derivations in this paper, and briefly review the theory about the barycentric form of unstructured systems (3). Then, we develop the structured barycentric forms in Section 3, followed by computational algorithms in Section 4 for the explicit construction of second-order systems (1) from frequency data. Section 5 illustrates the effectiveness of the presented methods for several numerical examples, including the vibrational responses of an underwater drone and bone tissue. The paper is concluded in Section 6.

2 Mathematical preliminaries and first-order systems analysis

For our derivation of the (structured) barycentric forms, the Sherman-Morrison-Woodbury formula for matrix inversion takes an essential role. Given an invertible matrix $\mathbf{X} \in \mathbb{C}^{r \times r}$ and two vectors $\mathbf{u}, \mathbf{v} \in \mathbb{C}^r$ such that $\mathbf{X} + \mathbf{u}\mathbf{v}^\top$ is also invertible, the Sherman-Morrison-Woodbury formula yields

$$\left(\mathbf{X} + \mathbf{u}\mathbf{v}^\top\right)^{-1} = \mathbf{X}^{-1} - \frac{\mathbf{X}^{-1}\mathbf{u}\mathbf{v}^\top\mathbf{X}^{-1}}{1 + \mathbf{v}^\top\mathbf{X}^{-1}\mathbf{u}}; \quad (5)$$

see, for example, [16]. In this work, we focus on transfer functions as in (2) and (4) where the inverse in the middle is pre- and post-multiplied by two vectors. Thus we consider the following adaption of (5).

Proposition 1. *Let $\mathbf{X} \in \mathbb{C}^{r \times r}$ be an invertible matrix and let $\mathbf{u}, \mathbf{v} \in \mathbb{C}^r$ be column vectors such that $\mathbf{X} + \mathbf{u}\mathbf{v}^\top$ is also invertible. Then, for any $\mathbf{z} \in \mathbb{C}^r$ it holds*

$$\mathbf{z}^\top \left(\mathbf{X} + \mathbf{u}\mathbf{v}^\top\right)^{-1} \mathbf{u} = \frac{\mathbf{z}^\top \mathbf{X}^{-1} \mathbf{u}}{1 + \mathbf{v}^\top \mathbf{X}^{-1} \mathbf{u}}. \quad (6)$$

Let $H(s)$ denote the transfer function of an unknown dynamical system. We assume that we have access to evaluations of the transfer function at *distinct* frequency points $\lambda_1, \dots, \lambda_r \in \mathbb{C}$ such that

$$H(\lambda_1) = h_1, \quad H(\lambda_2) = h_2, \quad \dots, \quad H(\lambda_r) = h_r. \quad (7)$$

We denote the complete data set of frequency points and transfer function values by $\{(\lambda_i, h_i) \mid 1 \leq i \leq r\}$.

Next, we consider the parametrization of first-order (*unstructured*) dynamical systems of the form (3) with the transfer function $\hat{H}(s) = \hat{\mathbf{c}}^\top (s\hat{\mathbf{E}} - \hat{\mathbf{A}})^{-1} \hat{\mathbf{b}}$ that interpolates the given data (7). In the following, the first-order dynamical system (3) of order r is denoted by $\hat{\Sigma}_{\text{FO}} : (\hat{\mathbf{E}}, \hat{\mathbf{A}}, \hat{\mathbf{b}}, \hat{\mathbf{c}})$. A slightly different proof of the next result can be found in [3] for the case of multi-input/multi-output dynamical systems. For thoroughness, we include a proof here as it will be the starting point for the structured variants considered later on.

Lemma 1. *Given the data (7), define*

$$\mathbf{\Lambda} = \text{diag}(\lambda_1, \dots, \lambda_r) \in \mathbb{C}^{r \times r} \quad \text{and} \quad \hat{\mathbf{c}} = [h_1 \quad h_2 \quad \dots \quad h_r]^\top \in \mathbb{C}^r,$$

and let $\mathbf{1}_r^\top = [1 \quad \dots \quad 1] \in \mathbb{C}^{1 \times r}$ be the vector of ones. If the first-order model $\hat{\Sigma}_{\text{FO}} : (\hat{\mathbf{E}}, \hat{\mathbf{A}}, \hat{\mathbf{b}}, \hat{\mathbf{c}})$ is constructed such that

$$\hat{\mathbf{E}}\mathbf{\Lambda} - \hat{\mathbf{A}} = \hat{\mathbf{b}}\mathbf{1}_r^\top \quad (8)$$

holds, where $\hat{\mathbf{b}} = [w_1 \quad \dots \quad w_r]^\top \in \mathbb{C}^r$ contains free parameters with $w_k \neq 0$, for $k = 1, \dots, r$, and the matrix $\hat{\mathbf{E}}$ is invertible, then the transfer function

$$\hat{H}(s) = \hat{\mathbf{c}}^\top (s\hat{\mathbf{E}} - \hat{\mathbf{A}})^{-1} \hat{\mathbf{b}} \quad (9)$$

of $\hat{\Sigma}_{\text{FO}}$ interpolates the data in (7), i.e., it holds

$$\hat{H}(\lambda_1) = h_1, \quad \hat{H}(\lambda_2) = h_2, \quad \dots, \quad \hat{H}(\lambda_r) = h_r. \quad (10)$$

Proof. Without loss of generality, we show the proof tailored specifically to the case $\hat{\mathbf{E}} = \mathbf{I}_r$. This scenario is by no means restrictive, since the matrix $\hat{\mathbf{E}}$ is considered to be invertible, and thus, can be incorporated into the matrices $\hat{\mathbf{A}}$ and $\hat{\mathbf{b}}$, accordingly. Let \mathbf{e}_i denote the i -th unit vector of length r . By multiplying the constraint in (8) with \mathbf{e}_i from the right, one obtains

$$(\mathbf{\Lambda} - \hat{\mathbf{A}})\mathbf{e}_i = \hat{\mathbf{b}}\mathbf{1}_r^\top \mathbf{e}_i$$

and, therefore,

$$(\lambda_i \mathbf{I}_r - \hat{\mathbf{A}})\mathbf{e}_i = \hat{\mathbf{b}}. \quad (11)$$

Note that since the entries of $\hat{\mathbf{b}}$ are nonzero, λ_i is not an eigenvalue of $\hat{\mathbf{A}}$. We prove this claim by contradiction. Let the entries of $\hat{\mathbf{b}}$ be nonzero and assume that λ_i is an eigenvalue of $\hat{\mathbf{A}}$ with the corresponding left eigenvector \mathbf{v} . Thus, it holds that

$$\mathbf{v}^\top (\mathbf{\Lambda} - \hat{\mathbf{b}}\mathbf{1}_r^\top - \lambda_i \mathbf{I}_r) = 0,$$

and, therefore,

$$\mathbf{v}^\top (\mathbf{\Lambda} - \lambda_i \mathbf{I}_r) = (\mathbf{v}^\top \hat{\mathbf{b}}) \mathbf{1}_r^\top = [\mathbf{v}^\top \hat{\mathbf{b}} \quad \mathbf{v}^\top \hat{\mathbf{b}} \quad \dots \quad \mathbf{v}^\top \hat{\mathbf{b}}].$$

Since the i -th entry of the row vector $\mathbf{v}^\top (\mathbf{\Lambda} - \lambda_i \mathbf{I}_r)$ is zero, we consequently have $\mathbf{v}^\top \hat{\mathbf{b}} = 0$, and thus $\mathbf{v}^\top (\mathbf{\Lambda} - \lambda_i \mathbf{I}_r) = \mathbf{0}$. Let $\mathbf{v} = [\alpha_1 \quad \alpha_2 \quad \dots \quad \alpha_r]^\top$. Since $\mathbf{\Lambda}$ is diagonal, it holds

$$\begin{aligned} & \mathbf{v}^\top (\mathbf{\Lambda} - \lambda_i \mathbf{I}_r) \\ &= [\alpha_1(\lambda_1 - \lambda_i) \quad \dots \quad \alpha_{i-1}(\lambda_{i-1} - \lambda_i) \quad 0 \quad \alpha_{i+1}(\lambda_{i+1} - \lambda_i) \quad \dots \quad \alpha_r(\lambda_r - \lambda_i)] \\ &= \mathbf{0}. \end{aligned}$$

Since the λ_k 's are assumed to be distinct, this implies $\alpha_1 = \dots = \alpha_{i-1} = \alpha_{i+1} = \dots = \alpha_r = 0$. Moreover, using $\mathbf{v}^\top \widehat{\mathbf{b}} = 0$, one obtains $\alpha_i w_i = 0$. But recall that $w_i \neq 0$; thus $\alpha_i = 0$ and, in summary, $\mathbf{v} = \mathbf{0}$. However, \mathbf{v} is an eigenvector, which leads to the contradiction. Therefore, λ_i is not an eigenvalue of $\widehat{\mathbf{A}}$. Since $\lambda_i \mathbf{I}_r - \widehat{\mathbf{A}}$ is invertible, Equation (11) yields $(\lambda_i \mathbf{I}_r - \widehat{\mathbf{A}})^{-1} \widehat{\mathbf{b}} = \mathbf{e}_i$. Then by multiplying this final relation with $\widehat{\mathbf{c}}^\top$ from the left, it holds $\widehat{\mathbf{c}}^\top (\lambda_i \mathbf{I}_r - \widehat{\mathbf{A}})^{-1} \widehat{\mathbf{b}} = \widehat{\mathbf{c}}^\top \mathbf{e}_i$, which proves the interpolation conditions (10). \square

In this work, we do not consider the case of systems $\widehat{\Sigma}_{\text{FO}}$ with differential-algebraic equations (descriptor systems), for which the matrix $\widehat{\mathbf{E}}$ is allowed to be singular. Such endeavors are kept for future research. Hence, in what follows we consider the matrix $\widehat{\mathbf{E}}$ to be invertible. For the simplicity of exposition, we choose without loss of generality the matrix $\widehat{\mathbf{E}}$ to be the $r \times r$ identity matrix \mathbf{I}_r , since any system $\widehat{\Sigma}_{\text{FO}}$ with $\widehat{\mathbf{E}}$ invertible can be equivalently written as $(\mathbf{I}_r, \widehat{\mathbf{E}}^{-1} \widehat{\mathbf{A}}, \widehat{\mathbf{E}}^{-1} \widehat{\mathbf{b}}, \widehat{\mathbf{c}})$. In this representation, one can observe that in the construction of $\widehat{\Sigma}_{\text{FO}}$ in (8), r parameters in $\widehat{\mathbf{b}}$ remain free to be chosen. They can, for example, be used to match further r interpolation conditions additionally to (10).

Using $\widehat{\mathbf{E}} = \mathbf{I}_r$, Equation (8) now reads $\mathbf{\Lambda} - \widehat{\mathbf{A}} = \widehat{\mathbf{b}} \mathbf{1}_r^\top$. Thus, substituting $\widehat{\mathbf{A}}$ into (9), the transfer function of $\widehat{\Sigma}_{\text{FO}}$ can be rewritten as

$$\widehat{H}(s) = \widehat{\mathbf{c}}^\top (s \mathbf{I}_r - \widehat{\mathbf{A}})^{-1} \widehat{\mathbf{b}} = \widehat{\mathbf{c}}^\top [s \mathbf{I}_r - (\mathbf{\Lambda} - \widehat{\mathbf{b}} \mathbf{1}_r^\top)]^{-1} \widehat{\mathbf{b}} = \widehat{\mathbf{c}}^\top [(s \mathbf{I}_r - \mathbf{\Lambda}) + \widehat{\mathbf{b}} \mathbf{1}_r^\top]^{-1} \widehat{\mathbf{b}}. \quad (12)$$

Define $\widehat{\Phi}(s) = s \mathbf{I}_r - \mathbf{\Lambda}$ to be the diagonal matrix function depending on the frequency parameter $s \in \mathbb{C}$. Then, the transfer function in (12) can be formulated as

$$\widehat{H}(s) = \widehat{\mathbf{c}}^\top (s \mathbf{I}_r - \widehat{\mathbf{A}})^{-1} \widehat{\mathbf{b}} = \widehat{\mathbf{c}}^\top (\widehat{\Phi}(s) + \widehat{\mathbf{b}} \mathbf{1}_r^\top)^{-1} \widehat{\mathbf{b}}. \quad (13)$$

The form of the transfer function $\widehat{H}(s)$ in terms of $\widehat{\Phi}(s)$ as given by (13) will play a crucial role in later sections to extend the interpolation theory to the structured case. The following result, which recovers the classical barycentric form of rational interpolants, follows from applying Lemma 1 to (13).

Corollary 1. *Given the interpolation data (7), the transfer function (13) of the first-order model that yields the interpolation conditions (10) can be equivalently expressed as*

$$\widehat{H}(s) = \frac{\widehat{\mathbf{c}}^\top \widehat{\Phi}(s)^{-1} \widehat{\mathbf{b}}}{1 + \mathbf{1}_r^\top \widehat{\Phi}(s)^{-1} \widehat{\mathbf{b}}}, \quad (14)$$

where $\widehat{\Phi}(s) = s \mathbf{I}_r - \mathbf{\Lambda}$, and $\mathbf{\Lambda}$, $\widehat{\mathbf{c}}$, and $\widehat{\mathbf{b}}$ are defined as in Lemma 1. This formula can be further represented as barycentric rational interpolation form

$$\widehat{H}(s) = \frac{\sum_{i=1}^r \frac{h_i w_i}{s - \lambda_i}}{1 + \sum_{i=1}^r \frac{w_i}{s - \lambda_i}}. \quad (15)$$

Proof. Applying the identity (6) in Proposition 1 to $\widehat{H}(s) = \widehat{\mathbf{c}}^\top (\widehat{\Phi}(s) + \widehat{\mathbf{b}} \mathbf{1}_r^\top)^{-1} \widehat{\mathbf{b}}$ using

$$\mathbf{u} = \widehat{\mathbf{b}}, \quad \mathbf{v} = \mathbf{1}_r, \quad \mathbf{z} = \widehat{\mathbf{c}}, \quad \mathbf{X} = \widehat{\Phi}(s)$$

yields (14). The fact that $\widehat{\Phi}(s)$ is diagonal and the definitions of $\widehat{\mathbf{b}}$ and $\widehat{\mathbf{c}}$ directly lead to

$$\widehat{\mathbf{c}}^\top \widehat{\Phi}(s)^{-1} \widehat{\mathbf{b}} = \sum_{i=1}^r \frac{h_i w_i}{(s - \lambda_i)} \quad \text{and} \quad \mathbf{1}_r^\top \widehat{\Phi}(s)^{-1} \widehat{\mathbf{b}} = \sum_{i=1}^r \frac{w_i}{(s - \lambda_i)},$$

which then together result in the barycentric form (15). \square

As stated earlier, the expression (15) is known as the barycentric form of the rational interpolant and is a well-studied object [9] as it forms the foundation for many rational approximation techniques [2, 24]. The derivation of the barycentric form in Corollary 1 follows a perspective from systems and control theory that aligns well with the second-order dynamics we study next.

The additional value of one in the denominator of (14) appears as a result of the Sherman-Morrison-Woodbury formula. Typically, in the classical theory about barycentric interpolation, such term does not appear in the denominator of the barycentric formula; see in particular [9, 24]. The rational function represented in (14) is strictly proper since the degree of the denominator is greater than the one of the numerator, which aligns with the setting of corresponding LTI systems. Although this may seem restrictive, the proposed approach can also accommodate proper rational functions corresponding to LTI systems with a nonzero feed-through term in the state-output equation.

3 Structured barycentric forms

As in the previous section, we assume to have transfer function measurements of the form (7) given and aim to construct models that fit the given data. However, in contrast to Section 2, we aim, from now on, to construct structured models of the form (1) denoted as $\widehat{\Sigma}_{\text{SO}} : (\widehat{\mathbf{M}}, \widehat{\mathbf{D}}, \widehat{\mathbf{K}}, \widehat{\mathbf{b}}, \widehat{\mathbf{c}})$, with the model matrices $\widehat{\mathbf{M}}, \widehat{\mathbf{D}}, \widehat{\mathbf{K}} \in \mathbb{R}^{r \times r}$ and $\widehat{\mathbf{b}}, \widehat{\mathbf{c}} \in \mathbb{R}^r$. Before we present the main results of this work, we introduce the following two sets of assumptions that will be needed later on.

Assumption 1. For the model matrices $\widehat{\Sigma}_{\text{SO}} : (\widehat{\mathbf{M}}, \widehat{\mathbf{D}}, \widehat{\mathbf{K}}, \widehat{\mathbf{b}}, \widehat{\mathbf{c}})$ and given data in (7), we assume that

$$(a) \text{ the matrix } \widehat{\mathbf{M}} \text{ is invertible, and} \tag{A1.1}$$

$$(b) \text{ the interpolation points } \{\lambda_1, \dots, \lambda_r\} \text{ are all distinct.} \tag{A1.2}$$

The reasons for imposing Assumptions (A1.1) and (A1.2) are similar to those in the case of first-order systems from the previous section. More specifically, Assumption (A1.1) enforces the system (1) to be described by ordinary differential equations rather than differential-algebraic ones, which require a singular $\widehat{\mathbf{M}}$. The modeling of such descriptor systems is left for future research. As in the first-order case, Assumption (A1.2) is necessary to avoid inconsistencies in the interpolation conditions. The case in which repeated interpolation points and derivative data are used for Hermite interpolation will be considered in a separate work.

Assumption 2. For the model matrices $\widehat{\Sigma}_{\text{SO}} : (\widehat{\mathbf{M}}, \widehat{\mathbf{D}}, \widehat{\mathbf{K}}, \widehat{\mathbf{b}}, \widehat{\mathbf{c}})$ and given data in (7), we assume for $i, k = 1, \dots, r$ and $i \neq k$ that either

$$(a) \text{ } -(\lambda_k + \lambda_i) \text{ is not an eigenvalue of the matrix } \widehat{\mathbf{M}}^{-1} \widehat{\mathbf{D}}, \text{ or} \tag{A2.1}$$

$$(b) \text{ } (\lambda_k \lambda_i) \text{ is not an eigenvalue of the matrix } \widehat{\mathbf{M}}^{-1} \widehat{\mathbf{K}}. \tag{A2.2}$$

In contrast to [Assumptions \(A1.1\)](#) and [\(A1.2\)](#), which need to hold both at the same time, only one of [Assumptions \(A2.1\)](#) and [\(A2.2\)](#) will be imposed at once, since these two assumptions are equivalent to each other for their respectively corresponding structured barycentric form, as it will become clearer later on. Although [Assumptions \(A2.1\)](#) and [\(A2.2\)](#) may seem restrictive at first glance, we will show that they occur naturally for practical choices of the parameters in the new structured barycentric forms. A more detailed discussion of this topic is provided in [Section 4.3](#).

3.1 Interpolatory second-order transfer functions

The following result extends [Lemma 1](#) to second-order systems establishing sufficient conditions for the interpolation of given transfer function data [\(7\)](#).

Lemma 2. *Given the interpolation data [\(7\)](#), define*

$$\mathbf{\Lambda} = \text{diag}(\lambda_1, \dots, \lambda_r) \in \mathbb{C}^{r \times r} \quad \text{and} \quad \widehat{\mathbf{c}} = [h_1 \ h_2 \ \dots \ h_r]^\top \in \mathbb{C}^r,$$

and let $\mathbf{1}_r^\top = [1 \ \dots \ 1] \in \mathbb{C}^{1 \times r}$ be the vector of ones. Let the second-order model $\widehat{\Sigma}_{\text{SO}} : (\widehat{\mathbf{M}}, \widehat{\mathbf{D}}, \widehat{\mathbf{K}}, \widehat{\mathbf{b}}, \widehat{\mathbf{c}})$ be constructed such that

$$\widehat{\mathbf{M}}\mathbf{\Lambda}^2 + \widehat{\mathbf{D}}\mathbf{\Lambda} + \widehat{\mathbf{K}} = \widehat{\mathbf{b}}\mathbf{1}_r^\top, \quad (16)$$

holds, where $\widehat{\mathbf{b}} = [w_1 \ \dots \ w_r]^\top \in \mathbb{C}^r$ contains free parameters with $w_k \neq 0$ for $k = 1, \dots, r$. If [Assumptions \(A1.1\)](#) and [\(A1.2\)](#) as well as either [Assumption \(A2.1\)](#) or [\(A2.2\)](#) hold, then the transfer function

$$\widehat{H}(s) = \widehat{\mathbf{c}}^\top (s^2 \widehat{\mathbf{M}} + s \widehat{\mathbf{D}} + \widehat{\mathbf{K}})^{-1} \widehat{\mathbf{b}}$$

of $\widehat{\Sigma}_{\text{SO}}$ interpolates the data in [\(7\)](#), i.e., it holds

$$\widehat{H}(\lambda_1) = h_1, \quad \widehat{H}(\lambda_2) = h_2, \quad \dots, \quad \widehat{H}(\lambda_r) = h_r. \quad (17)$$

Proof. Without loss of generality, we show the proof tailored specifically to the case $\widehat{\mathbf{M}} = \mathbf{I}_r$. This scenario is by no means restrictive, since the $\widehat{\mathbf{M}}$ matrix is considered to be invertible; see [Assumption \(A1.1\)](#). Thus, it can be incorporated into $\widehat{\mathbf{D}}$, $\widehat{\mathbf{K}}$ and $\widehat{\mathbf{b}}$, accordingly. For the consideration of eigenvalues of second-order systems, we introduce the augmented matrices

$$\mathcal{E} = \begin{bmatrix} \mathbf{I}_r & 0 \\ 0 & \widehat{\mathbf{M}} \end{bmatrix} = \mathbf{I}_{2r}, \quad \mathcal{A} = \begin{bmatrix} 0 & \mathbf{I}_r \\ -\widehat{\mathbf{K}} & -\widehat{\mathbf{D}} \end{bmatrix}. \quad (18)$$

Since the entries of $\widehat{\mathbf{b}}$ are nonzero and with [Assumption \(A2.1\)](#) that $-(\lambda_k + \lambda_i)$ is not an eigenvalue of matrix $\widehat{\mathbf{D}}$, the interpolation point λ_i is not a solution to the linearized eigenvalue problem of the matrix pencil $(\mathcal{A}, \mathcal{E})$ in [\(18\)](#), i.e., it is not an eigenvalue of the quadratic pencil involving $\widehat{\mathbf{M}}$, $\widehat{\mathbf{D}}$ and $\widehat{\mathbf{K}}$. We prove this claim by contradiction. Let the entries of $\widehat{\mathbf{b}}$ be nonzero and assume that λ_i is an eigenvalue of \mathcal{A} with the corresponding left-eigenvector $\mathbf{v}^\top = [\mathbf{v}_1^\top \ \mathbf{v}_2^\top]$. Thus, it holds

$$[\mathbf{v}_1^\top \ \mathbf{v}_2^\top] (\lambda_i \mathcal{E} - \mathcal{A}) = \mathbf{0}.$$

Employing the block matrix structure from [\(18\)](#) yields the quadratic eigenvalue relation

$$\lambda_i^2 \mathbf{v}_2^\top \mathbf{I}_r + \lambda_i \mathbf{v}_2^\top \widehat{\mathbf{D}} + \mathbf{v}_2^\top \widehat{\mathbf{K}} = \mathbf{0}. \quad (19)$$

By multiplying the constraint in (16) with \mathbf{e}_i from the right, we obtain for $1 \leq i \leq k$ that

$$(\lambda_i^2 \mathbf{I}_r + \widehat{\mathbf{D}}\lambda_i + \widehat{\mathbf{K}})\mathbf{e}_i = \widehat{\mathbf{b}}. \quad (20)$$

Then, multiplication of this last equation (20) with \mathbf{v}_2^\top from the left yields

$$\lambda_i^2 \mathbf{v}_2^\top \mathbf{e}_i + \lambda_i \mathbf{v}_2^\top \widehat{\mathbf{D}}\mathbf{e}_i + \mathbf{v}_2^\top \widehat{\mathbf{K}}\mathbf{e}_i = \mathbf{v}_2^\top \widehat{\mathbf{b}}. \quad (21)$$

It follows directly from (19) and (21) that $\mathbf{v}_2^\top \widehat{\mathbf{b}} = \mathbf{0}$. Let the eigenvector be given as $\mathbf{v}_2 = [\alpha_1 \ \alpha_2 \ \dots \ \alpha_r]^\top$. Without loss of generality assume that $\widehat{\mathbf{D}}$ is a diagonal matrix with $\widehat{\mathbf{D}} = \text{diag}(\delta_1, \dots, \delta_r)$. Now we use (16) to describe the stiffness matrix $\widehat{\mathbf{K}}$ in terms of the rest such that $\widehat{\mathbf{K}} = \widehat{\mathbf{b}}\mathbf{1}_r^\top - \widehat{\mathbf{D}}\mathbf{\Lambda} - \mathbf{\Lambda}^2$ and substitute this relation into (19) to obtain

$$\begin{aligned} \mathbf{0} &= \lambda_i^2 \mathbf{v}_2^\top + \lambda_i \mathbf{v}_2^\top \widehat{\mathbf{D}} + \mathbf{v}_2^\top (\widehat{\mathbf{b}}\mathbf{1}_r^\top - \widehat{\mathbf{D}}\mathbf{\Lambda} - \mathbf{\Lambda}^2) \\ &= \mathbf{v}_2^\top \widehat{\mathbf{D}}(\lambda_i \mathbf{I}_r - \mathbf{\Lambda}) + \mathbf{v}_2^\top (\lambda_i^2 \mathbf{I}_r - \mathbf{\Lambda}^2) + \underbrace{\mathbf{v}_2^\top \widehat{\mathbf{b}} \mathbf{1}_r^\top}_{=0} \\ &= \mathbf{v}_2^\top (\widehat{\mathbf{D}} + \lambda_i \mathbf{I}_r + \mathbf{\Lambda})(\lambda_i \mathbf{I}_r - \mathbf{\Lambda}) \\ &= [\alpha_1(\delta_1 + \lambda_1 + \lambda_i)(\lambda_1 - \lambda_i) \ \dots \ 0 \ \dots \ \alpha_r(\delta_r + \lambda_r + \lambda_i)(\lambda_r - \lambda_i)]. \end{aligned}$$

Since the λ_k 's are distinct (Assumption (A1.2)) and $\delta_k + \lambda_k + \lambda_i \neq 0$ for all $1 \leq k \leq r$ due to Assumption (A2.1), it implies that $\alpha_1 = \dots = \alpha_{i-1} = \alpha_{i+1} = \dots = \alpha_r = 0$. Moreover, using $\mathbf{v}_2^\top \widehat{\mathbf{b}} = 0$, it holds that $\alpha_i w_i = 0$. Since $w_i \neq 0$, this would imply $\alpha_i = 0$, yielding $\mathbf{v}_2 = \mathbf{0}$. However, \mathbf{v}_2 is an eigenvector, thus leading to the contradiction. Therefore, λ_i is not a solution to the quadratic eigenvalue problem.

As a results, the matrix $\lambda_i^2 \mathbf{I}_r + \lambda_i \widehat{\mathbf{D}} + \widehat{\mathbf{K}}$ is non-singular, and by multiplying (20) with $(\mathbf{I}_r \lambda_i^2 + \widehat{\mathbf{D}}\lambda_i + \widehat{\mathbf{K}})^{-1}$ from the left, we get

$$(\mathbf{I}_r \lambda_i^2 + \widehat{\mathbf{D}}\lambda_i + \widehat{\mathbf{K}})^{-1} \widehat{\mathbf{b}} = \mathbf{e}_i$$

and, therefore,

$$\widehat{\mathbf{c}}^\top (\mathbf{I}_r \lambda_i^2 + \widehat{\mathbf{D}}\lambda_i + \widehat{\mathbf{K}})^{-1} \widehat{\mathbf{b}} = \widehat{\mathbf{c}}^\top \mathbf{e}_i = h_i.$$

Hence, we have shown that $\widehat{H}(\lambda_i) = h_i$ for any $1 \leq i \leq r$. Note that we only used (A2.1) out of Assumption 2 in this proof, which allowed the description of the stiffness matrix $\widehat{\mathbf{K}}$ by the other terms in (16). An analogous proof relies on Assumption (A2.2), which allows the reformulation of (16) for the damping matrix $\widehat{\mathbf{D}}$. Due to the similarity to the presented proof, we omit this part. \square

Similar to the case of first-order systems in Section 2, we can eliminate one of the unknown matrices in the constraint (16) by using Assumption (A1.1). Thereby, we will choose the mass matrix to be the r -dimensional identity matrix, $\widehat{\mathbf{M}} = \mathbf{I}_r$. However, in contrast to the case of first-order systems, this leaves us with three remaining unknown matrices in (16) instead of two. Following diagonalization assumptions, which we will point out later in detail, this leaves us with $2r$ free parameters to choose for the explicit realization of interpolating second-order systems.

Remark 1. Aside from this work, a data-driven method for the derivation of structured models with interpolating transfer functions has been developed in [36]. Therein, the authors use constraints similar to (16) to parametrize the model matrices as the solution of large-scale linear systems of equations to enforce the interpolation conditions.

The unknowns in these linear systems correspond to the entries of the vectorized state-space quantities. There is no discussion of or connection to structured barycentric forms in [36] (which represents the main novelty of the current work) as [36] is directly related to and based on the *non-barycentric* Loewner framework for interpolation [22] and the projection-based interpolatory model reduction of structured systems [6]. However, it will be interesting to revisit [36] in a future work since it might provide directions for extending the barycentric form to different structures than those we consider here.

In the following derivation of structured barycentric forms, we will make use of the equality constraint in (16) that enforces r interpolation conditions. As mentioned above, the remaining free $2r$ parameters are given in the input vector $\hat{\mathbf{b}}$ and either in the stiffness matrix $\hat{\mathbf{K}}$ or damping matrix $\hat{\mathbf{D}}$. Therefore, different barycentric forms result from the reformulation of (16) in terms of either stiffness (in Section 3.2) or damping matrix (in Section 3.3).

3.2 Parametrization with constrained stiffness matrix

3.2.1 General setup

In this section, we incorporate the remaining free parameters of the system $\hat{\Sigma}_{\text{SO}}$ into the damping matrix $\hat{\mathbf{D}}$ and the input vector $\hat{\mathbf{b}}$. Therefore, from (16) it follows that the stiffness matrix satisfies

$$\hat{\mathbf{K}} = \hat{\mathbf{b}}\mathbf{1}_r^\top - \hat{\mathbf{M}}\mathbf{\Lambda}^2 - \hat{\mathbf{D}}\mathbf{\Lambda}. \quad (22)$$

Substituting (22) into the transfer function $\hat{H}(s)$ corresponding to the second-order model $\hat{\Sigma}_{\text{SO}} : (\hat{\mathbf{M}}, \hat{\mathbf{D}}, \hat{\mathbf{K}}, \hat{\mathbf{b}}, \hat{\mathbf{c}})$ yields

$$\begin{aligned} \hat{H}(s) &= \hat{\mathbf{c}}^\top (s^2 \hat{\mathbf{M}} + s \hat{\mathbf{D}} + \hat{\mathbf{K}})^{-1} \hat{\mathbf{b}} \\ &= \hat{\mathbf{c}}^\top (s^2 \hat{\mathbf{M}} + s \hat{\mathbf{D}} + \hat{\mathbf{b}}\mathbf{1}_r^\top - \hat{\mathbf{M}}\mathbf{\Lambda}^2 - \hat{\mathbf{D}}\mathbf{\Lambda})^{-1} \hat{\mathbf{b}} \\ &= \hat{\mathbf{c}}^\top (\hat{\mathbf{\Phi}}(s) + \hat{\mathbf{b}}\mathbf{1}_r^\top)^{-1} \hat{\mathbf{b}}, \end{aligned} \quad (23)$$

where the matrix-valued function $\hat{\mathbf{\Phi}}(s)$ is given by

$$\begin{aligned} \hat{\mathbf{\Phi}}(s) &= s^2 \hat{\mathbf{M}} + s \hat{\mathbf{D}} - \hat{\mathbf{M}}\mathbf{\Lambda}^2 - \hat{\mathbf{D}}\mathbf{\Lambda} \\ &= \hat{\mathbf{M}}(s^2 \mathbf{I}_r - \mathbf{\Lambda}^2) + \hat{\mathbf{D}}(s \mathbf{I}_r - \mathbf{\Lambda}) \\ &= \left(\hat{\mathbf{M}}(s \mathbf{I}_r + \mathbf{\Lambda}) + \hat{\mathbf{D}} \right) (s \mathbf{I}_r - \mathbf{\Lambda}). \end{aligned}$$

The following lemma states the structured barycentric form of (23) in terms of the input and output vectors, and the matrix-valued function $\hat{\mathbf{\Phi}}(s)$.

Lemma 3. *Given the interpolation data (7), the transfer function (23) of the second-order model that yields the interpolation conditions (17) can be equivalently expressed as*

$$\hat{H}(s) = \frac{\hat{\mathbf{c}}^\top \hat{\mathbf{\Phi}}(s)^{-1} \hat{\mathbf{b}}}{1 + \mathbf{1}_r^\top \hat{\mathbf{\Phi}}(s)^{-1} \hat{\mathbf{b}}},$$

where $\hat{\mathbf{\Phi}}(s) = \left(\hat{\mathbf{M}}(s \mathbf{I}_r + \mathbf{\Lambda}) + \hat{\mathbf{D}} \right) (s \mathbf{I}_r - \mathbf{\Lambda})$, and $\mathbf{\Lambda}$, $\hat{\mathbf{c}}$, and $\hat{\mathbf{b}}$ are as defined in Lemma 1.

Proof. Using Proposition 1 for the formulation of $\hat{H}(s)$ in (23), with the following choice of vectors and matrices

$$\mathbf{u} = \hat{\mathbf{b}}, \quad \mathbf{v} = \mathbf{1}_r, \quad \mathbf{z} = \hat{\mathbf{c}}, \quad \mathbf{X} = \hat{\mathbf{\Phi}}(s)$$

yields the result of the lemma. \square

As mentioned in [Section 3.1](#), we choose the mass matrix $\widehat{\mathbf{M}}$ to be the identity due to [Assumption \(A1.1\)](#). Under the assumption that $\widehat{\mathbf{D}}$ has no higher order Jordan blocks, it can be diagonalized while preserving $\widehat{\mathbf{M}} = \mathbf{I}_r$ such that

$$\widehat{\mathbf{D}} = \text{diag}(\delta_1, \dots, \delta_r) \quad \text{and} \quad \widehat{\mathbf{M}} = \mathbf{I}_r = \text{diag}(1, \dots, 1).$$

In this case, the matrix-valued function $\widehat{\Phi}(s)$ is a diagonal matrix for all $s \in \mathbb{C}$, which allows us to write

$$\begin{aligned} \widehat{\Phi}(s) &= \left(\widehat{\mathbf{M}}(s\mathbf{I}_r + \mathbf{\Lambda}) + \widehat{\mathbf{D}} \right) (s\mathbf{I}_r - \mathbf{\Lambda}) \\ &= \text{diag} \left((s - \lambda_1)(s + \lambda_1 + \delta_1), \dots, (s - \lambda_r)(s + \lambda_r + \delta_r) \right). \end{aligned} \quad (24)$$

Using this diagonal form of the matrix-valued function in [Lemma 3](#) yields the following result: a structured barycentric formula for second-order transfer functions.

Theorem 1. *Given interpolation points and measurements $\{(\lambda_i, h_i) \mid 1 \leq i \leq r\}$ and let [Assumptions \(A1.1\)](#) and [\(A1.2\)](#) as well as [Assumption \(A2.1\)](#) hold. The barycentric form of the transfer function $\widehat{H}(s)$ corresponding to second-order system $\widehat{\Sigma}_{\text{SO}} : (\widehat{\mathbf{M}}, \widehat{\mathbf{D}}, \widehat{\mathbf{K}}, \widehat{\mathbf{b}}, \widehat{\mathbf{c}})$ is given by*

$$\widehat{H}(s) = \frac{\sum_{i=1}^r \frac{h_i w_i}{(s - \lambda_i)(s - \sigma_i)}}{1 + \sum_{i=1}^r \frac{w_i}{(s - \lambda_i)(s - \sigma_i)}}, \quad (25)$$

with the weights $0 \neq w_i \in \mathbb{C}$ and support points $\sigma_i = -(\delta_i + \lambda_i)$, where $\delta_i \in \mathbb{C}$ are damping parameters, for $1 \leq i \leq r$. The barycentric form [\(25\)](#) satisfies the interpolation conditions [\(17\)](#). The matrices of the corresponding second-order system are given by

$$\begin{aligned} \widehat{\mathbf{M}} &= \mathbf{I}_r, & \widehat{\mathbf{D}} &= -\text{diag}(\lambda_1 + \sigma_1, \dots, \lambda_r + \sigma_r), \\ \widehat{\mathbf{K}} &= \widehat{\mathbf{b}}\mathbf{1}_r^\top - \mathbf{\Lambda}^2 - \widehat{\mathbf{D}}\mathbf{\Lambda}, & \widehat{\mathbf{b}} &= [w_1 \quad \dots \quad w_r]^\top, \\ \widehat{\mathbf{c}} &= [h_1 \quad \dots \quad h_r]^\top. \end{aligned} \quad (26)$$

Proof. By making use of the diagonal structure of $\widehat{\Phi}(s)$ in [\(24\)](#) and the other components

$$\mathbf{1}_r = [1 \quad \dots \quad 1]^\top, \quad \widehat{\mathbf{b}} = [w_1 \quad \dots \quad w_r]^\top, \quad \widehat{\mathbf{c}} = [h_1 \quad \dots \quad h_r]^\top$$

in the formulation of the transfer function in [Lemma 3](#), the transfer function is rewritten in barycentric form by multiplying out the matrix-vector products as

$$\widehat{H}(s) = \frac{\widehat{\mathbf{c}}^\top \widehat{\Phi}(s)^{-1} \widehat{\mathbf{b}}}{1 + \mathbf{1}_r^\top \widehat{\Phi}(s)^{-1} \widehat{\mathbf{b}}} = \frac{\sum_{i=1}^r \frac{h_i w_i}{(s - \lambda_i)(s + \lambda_i + \delta_i)}}{1 + \sum_{i=1}^r \frac{w_i}{(s - \lambda_i)(s + \lambda_i + \delta_i)}}.$$

Setting the support points $\sigma_i = -(\delta_i + \lambda_i)$, the result in [\(25\)](#) follows directly. The realization [\(26\)](#) is then given by rearranging the different parameters into the corresponding matrices and vectors. \square

Note that given the notation $\Sigma = \text{diag}(\sigma_1, \dots, \sigma_r)$, the realization in (26) can equivalently be written as

$$\begin{aligned}\widehat{\mathbf{M}} &= \mathbf{I}_r, & \widehat{\mathbf{D}} &= -\mathbf{\Lambda} - \Sigma, \\ \widehat{\mathbf{K}} &= \widehat{\mathbf{b}}\mathbf{1}_r^\top + \mathbf{\Lambda}\Sigma, & \widehat{\mathbf{b}} &= [w_1 \ \dots \ w_r]^\top, \\ \widehat{\mathbf{c}} &= [h_1 \ \dots \ h_r]^\top.\end{aligned}$$

The free parameters that explicitly appear above are $2r$ in total and are given by the entries of the vector $\widehat{\mathbf{b}}$ and of the diagonal matrix Σ , i.e., the free parameters in the structured barycentric form (25) are $\{w_1, \dots, w_r\} \cup \{\sigma_1, \dots, \sigma_r\}$.

3.2.2 Systems with zero damping matrix

An important subclass of second-order systems (1) is given by a zero damping matrix, i.e., $\mathbf{D} = 0$. These occur, for example, in the case of “conservative” dynamics where no dissipation/damping is considered. Hamiltonian systems belong to this category [1, 23]. Retaining this additional structure allows, for example, modeling the preservation of energy in the system. Another problem class that can be modeled by a zero damping matrix is the case of hysteretic damping, i.e., constant damping over the complete frequency range [5, 13]. This is used, for example, to model the general influence of physical structures on the damping behavior of systems. Thereby, the damping matrix is considered to be frequency dependent with $\mathbf{D}(s) = \frac{1}{s}i\eta\mathbf{K}$. Inserting this damping definition into the second-order transfer function (2) yields

$$H(s) = \mathbf{c}^\top \left(s^2 \mathbf{M} + \frac{s}{s} i\eta \mathbf{K} + \mathbf{K} \right)^{-1} \mathbf{b} = \mathbf{c}^\top (s^2 \mathbf{M} + (1 + i\eta) \mathbf{K})^{-1} \mathbf{b},$$

which can be seen as a system with a complex stiffness matrix and zero damping matrix. The following corollary refines the results from Theorem 1 to the case of system structure with zero damping matrix, $\widehat{\mathbf{D}} = \mathbf{0}$.

Corollary 2. *Given interpolation points and measurements $\{(\lambda_i, h_i) \mid 1 \leq i \leq r\}$ and let Assumptions (A1.1) and (A1.2) as well as Assumption (A2.1) hold. The barycentric form of the transfer function $\widehat{H}(s)$ corresponding to second-order system $\widehat{\Sigma}_{\text{SO}} : (\widehat{\mathbf{M}}, \mathbf{0}, \widehat{\mathbf{K}}, \widehat{\mathbf{b}}, \widehat{\mathbf{c}})$ is given by*

$$\widehat{H}(s) = \frac{\sum_{i=1}^r \frac{h_i w_i}{s^2 - \lambda_i^2}}{1 + \sum_{i=1}^r \frac{w_i}{s^2 - \lambda_i^2}}, \quad (27)$$

with the weights $0 \neq w_i \in \mathbb{C}$, for $1 \leq i \leq r$. The barycentric form (27) satisfies the interpolation conditions (17) and it can be written as a second-order dynamical systems with zero damping, i.e.,

$$\widehat{H}(s) = \widehat{\mathbf{c}}^\top (s^2 \widehat{\mathbf{M}} + \widehat{\mathbf{K}})^{-1} \widehat{\mathbf{b}},$$

where

$$\widehat{\mathbf{M}} = \mathbf{I}_r, \quad \widehat{\mathbf{K}} = \widehat{\mathbf{b}}\mathbf{1}_r^\top - \mathbf{\Lambda}^2, \quad \widehat{\mathbf{b}} = [w_1 \ \dots \ w_r]^\top, \quad \widehat{\mathbf{c}} = [h_1 \ \dots \ h_r]^\top.$$

As in Theorem 1, Assumption (A2.1) needs to hold for (27) to satisfy the interpolation conditions (17). However, in the special case of $\widehat{\mathbf{D}} = \mathbf{0}$, Assumption (A2.1) simplifies to $\lambda_i \neq -\lambda_k$, for all $i \neq k$. In particular, if the interpolation points are chosen on the imaginary axis, no complex conjugate pairs are allowed in the set of interpolation points.

3.3 Parametrization with constrained damping matrix

In this section, we incorporate the remaining free parameters of the system $\widehat{\Sigma}_{\text{SO}}$ into the stiffness matrix $\widehat{\mathbf{K}}$ and the input vector $\widehat{\mathbf{b}}$. Therefore, it follows from (16) that the damping matrix satisfies

$$\widehat{\mathbf{D}}\boldsymbol{\Lambda} = \widehat{\mathbf{b}}\mathbf{1}_r^\top - \widehat{\mathbf{M}}\boldsymbol{\Lambda}^2 - \widehat{\mathbf{K}}. \quad (28)$$

Under the assumption that $\boldsymbol{\Lambda}$ is invertible, i.e., zero is not an interpolation point, one can equivalently write (28) as

$$\widehat{\mathbf{D}} = \widehat{\mathbf{b}}\mathbf{1}_r^\top \boldsymbol{\Lambda}^{-1} - \widehat{\mathbf{M}}\boldsymbol{\Lambda} - \widehat{\mathbf{K}}\boldsymbol{\Lambda}^{-1}. \quad (29)$$

By substituting (29) into the formula of the transfer function $\widehat{H}(s)$ corresponding to the second-order model $\widehat{\Sigma}_{\text{SO}} : (\widehat{\mathbf{M}}, \widehat{\mathbf{D}}, \widehat{\mathbf{K}}, \widehat{\mathbf{b}}, \widehat{\mathbf{c}})$, it holds

$$\begin{aligned} \widehat{H}(s) &= \widehat{\mathbf{c}}^\top (s^2 \widehat{\mathbf{M}} + s \widehat{\mathbf{D}} + \widehat{\mathbf{K}})^{-1} \widehat{\mathbf{b}} \\ &= \widehat{\mathbf{c}}^\top \left(s^2 \widehat{\mathbf{M}} + s \left(\widehat{\mathbf{b}}\mathbf{1}_r^\top \boldsymbol{\Lambda}^{-1} - \widehat{\mathbf{M}}\boldsymbol{\Lambda} - \widehat{\mathbf{K}}\boldsymbol{\Lambda}^{-1} \right) + \widehat{\mathbf{K}} \right)^{-1} \widehat{\mathbf{b}} \\ &= \widehat{\mathbf{c}}^\top \left(\widehat{\mathbf{M}}(s^2 \mathbf{I}_r - s\boldsymbol{\Lambda}) + \widehat{\mathbf{K}}(\mathbf{I}_r - s\boldsymbol{\Lambda}^{-1}) + s\widehat{\mathbf{b}}\mathbf{1}_r^\top \boldsymbol{\Lambda}^{-1} \right)^{-1} \widehat{\mathbf{b}} \\ &= \widehat{\mathbf{c}}^\top \left(\widehat{\Psi}(s) + s\widehat{\mathbf{b}}\mathbf{1}_r^\top \boldsymbol{\Lambda}^{-1} \right)^{-1} \widehat{\mathbf{b}}, \end{aligned} \quad (30)$$

where the matrix-valued function $\widehat{\Psi}(s)$ is given by

$$\begin{aligned} \widehat{\Psi}(s) &= \widehat{\mathbf{M}}(s^2 \mathbf{I}_r - s\boldsymbol{\Lambda}) + \widehat{\mathbf{K}}(\mathbf{I}_r - s\boldsymbol{\Lambda}^{-1}) \\ &= (s\widehat{\mathbf{M}} - \widehat{\mathbf{K}}\boldsymbol{\Lambda}^{-1})(s\mathbf{I}_r - \boldsymbol{\Lambda}). \end{aligned}$$

Similar to Lemma 3, the following lemma states the structured barycentric form of (30) in terms of the input and output vectors and the matrix-valued function $\widehat{\Phi}(s)$.

Lemma 4. *Given the interpolation data (7), the transfer function (30) of the second-order model that yields the interpolation conditions (17) can be equivalently expressed as*

$$\widehat{H}(s) = \frac{\widehat{\mathbf{c}}^\top \widehat{\Psi}(s)^{-1} \widehat{\mathbf{b}}}{1 + s\widehat{\mathbf{f}}^\top \widehat{\Psi}(s)^{-1} \widehat{\mathbf{b}}}$$

where $\widehat{\Psi}(s) = (s\widehat{\mathbf{M}} - \widehat{\mathbf{K}}\boldsymbol{\Lambda}^{-1})(s\mathbf{I}_r - \boldsymbol{\Lambda})$, $\widehat{\mathbf{f}} = \boldsymbol{\Lambda}^{-1}\mathbf{1}_r$ and $\boldsymbol{\Lambda}$, $\widehat{\mathbf{c}}$, and $\widehat{\mathbf{b}}$ are defined as in Lemma 1.

Proof. As previously done in the proof of Lemma 3, we apply Proposition 1 to the formulation of $\widehat{H}(s)$ in (30), with the following choice of vectors and matrices

$$\mathbf{u} = \widehat{\mathbf{b}}, \quad \mathbf{v} = s\widehat{\mathbf{f}} = s\boldsymbol{\Lambda}^{-1}\mathbf{1}_r, \quad \mathbf{z} = \widehat{\mathbf{c}}, \quad \mathbf{X} = \widehat{\Psi}(s),$$

which yields the result of the lemma. \square

As in Section 3.2, we can assume that the mass matrix $\widehat{\mathbf{M}}$ to be the identity due to Assumption (A1.1). However, this time, we additionally assume that $\widehat{\mathbf{K}}$ has no higher order Jordan blocks such that we can diagonalize the stiffness matrix while preserving the identity mass matrix

$$\widehat{\mathbf{K}} = \text{diag}(\kappa_1, \dots, \kappa_r) \quad \text{and} \quad \widehat{\mathbf{M}} = \mathbf{I}_r = \text{diag}(1, \dots, 1).$$

Therefore, the matrix-valued function $\widehat{\Psi}(s)$ is a diagonal matrix for all $s \in \mathbb{C}$, which can be written as

$$\begin{aligned}\widehat{\Phi}(s) &= (s\widehat{M} - \widehat{K}\Lambda^{-1})(s\mathbf{I}_r - \Lambda) \\ &= \text{diag}\left((s - \lambda_1)(s - \kappa_1\lambda_1^{-1}), \dots, (s - \lambda_r)(s - \kappa_r\lambda_r^{-1})\right).\end{aligned}\quad (31)$$

Using this diagonal form of the matrix-valued function in [Lemma 4](#) yields the barycentric form for the constrained damping case.

Theorem 2. *Given interpolation points and measurements $\{(\lambda_i, h_i) \mid 1 \leq i \leq r\}$, let [Assumptions \(A1.1\)](#) and [\(A1.2\)](#) as well as [Assumption \(A2.2\)](#) hold. The barycentric form of the transfer function $\widehat{H}(s)$ corresponding to second-order system $\widehat{\Sigma}_{\text{SO}} : (\widehat{M}, \widehat{D}, \widehat{K}, \widehat{\mathbf{b}}, \widehat{\mathbf{c}})$ is given by*

$$\widehat{H}(s) = \frac{\sum_{i=1}^r \frac{h_i w_i}{(s - \lambda_i)(s - \theta_i)}}{1 + \sum_{i=1}^r \frac{s w_i \lambda_i^{-1}}{(s - \lambda_i)(s - \theta_i)}}, \quad (32)$$

with the weights $0 \neq w_i \in \mathbb{C}$ and support points $\theta_i = \kappa_i \lambda_i^{-1}$, where $\kappa_i \in \mathbb{C}$ are stiffness parameters, for $1 \leq i \leq r$. The barycentric form [\(32\)](#) satisfies the interpolation conditions [\(17\)](#). Moreover, the matrices of the corresponding second-order system are given as

$$\begin{aligned}\widehat{M} &= \mathbf{I}_r, & \widehat{D} &= \widehat{\mathbf{b}}\mathbf{1}_r^T \Lambda^{-1} - \Lambda - \widehat{K}\Lambda^{-1}, \\ \widehat{K} &= \text{diag}(\theta_1 \lambda_1, \dots, \theta_r \lambda_r), & \widehat{\mathbf{b}} &= [w_1 \ \dots \ w_r]^T, \\ \widehat{\mathbf{c}} &= [h_1 \ \dots \ h_r]^T.\end{aligned}\quad (33)$$

Proof. By using the diagonal structure of $\widehat{\Psi}(s)$ in [\(31\)](#), and the structure of the other components

$$\widehat{\mathbf{f}} = \Lambda^{-1} \mathbf{1}_r = [\lambda_1^{-1} \ \dots \ \lambda_r^{-1}]^T, \quad \widehat{\mathbf{b}} = [w_1 \ \dots \ w_r]^T, \quad \widehat{\mathbf{c}} = [h_1 \ \dots \ h_r]^T,$$

in the formulation of the transfer function in [Lemma 4](#), the transfer function is rewritten in barycentric form by multiplying out the matrix-vector products as

$$\widehat{H}(s) = \frac{\widehat{\mathbf{c}}^T \widehat{\Psi}(s)^{-1} \widehat{\mathbf{b}}}{1 + \widehat{\mathbf{f}}^T \widehat{\Psi}(s)^{-1} \widehat{\mathbf{b}}} = \frac{\sum_{i=1}^r \frac{h_i w_i}{(s - \lambda_i)(s - \kappa_i \lambda_i^{-1})}}{1 + \sum_{i=1}^r \frac{s w_i \lambda_i^{-1}}{(s - \lambda_i)(s - \kappa_i \lambda_i^{-1})}}.$$

Setting the support points $\theta_i = \kappa_i \lambda_i^{-1}$, the result in [\(32\)](#) follows directly. The realization [\(33\)](#) is then given by rearranging the different parameters into the corresponding matrices and vectors. \square

As for the realization of matrices in [Theorem 1](#), the matrices in [\(33\)](#) can be reformulated by introducing the notation $\Theta = \text{diag}(\theta_1, \dots, \theta_r)$ such that

$$\begin{aligned}\widehat{M} &= \mathbf{I}_r, & \widehat{D} &= \widehat{\mathbf{b}}\mathbf{1}_r^T \Lambda^{-1} - \Lambda - \Theta, \\ \widehat{K} &= \Theta \Lambda, & \widehat{\mathbf{b}} &= [w_1 \ \dots \ w_r]^T, \\ \widehat{\mathbf{c}} &= [h_1 \ \dots \ h_r]^T.\end{aligned}$$

Algorithm 1: Linearized K -constrained second-order barycentric Loewner framework.

Input: Left and right interpolation data $\{(\lambda_i, h_i) \mid 1 \leq i \leq r\}$ and $\{(\mu_i, g_i) \mid 1 \leq i \leq r\}$, support points $\sigma_1, \dots, \sigma_r \in \mathbb{C}$.

Output: Second-order system matrices $\widehat{\mathbf{M}}, \widehat{\mathbf{D}}, \widehat{\mathbf{K}}, \widehat{\mathbf{b}}, \widehat{\mathbf{c}}$.

1 Construct the r -dimensional divided differences matrix

$$\mathbf{L}_K = \begin{bmatrix} \frac{h_1 - g_1}{(\mu_1 - \lambda_1)(\mu_1 - \sigma_1)} & \cdots & \frac{h_r - g_1}{(\mu_1 - \lambda_r)(\mu_1 - \sigma_r)} \\ \vdots & \ddots & \vdots \\ \frac{h_1 - g_r}{(\mu_r - \lambda_1)(\mu_r - \sigma_1)} & \cdots & \frac{h_r - g_r}{(\mu_r - \lambda_r)(\mu_r - \sigma_r)} \end{bmatrix}.$$

2 Solve the linear system of equations $\mathbf{L}_K \mathbf{w} = \mathbf{g}$, for the unknown weights

$$\mathbf{w} = [w_1 \ \dots \ w_r]^\top \text{ and the given data } \mathbf{g} = [g_1 \ \dots \ g_r]^\top.$$

3 Construct the second-order system matrices

$$\widehat{\mathbf{M}} = \mathbf{I}_r, \quad \widehat{\mathbf{D}} = -\mathbf{\Lambda} - \mathbf{\Sigma}, \quad \widehat{\mathbf{K}} = \widehat{\mathbf{b}}\mathbf{1}_r^\top + \mathbf{\Lambda}\mathbf{\Sigma}, \quad \widehat{\mathbf{b}} = \mathbf{w}, \quad \widehat{\mathbf{c}} = [h_1 \ \dots \ h_r]^\top,$$

$$\text{with } \mathbf{\Lambda} = \text{diag}(\lambda_1, \dots, \lambda_r) \text{ and } \mathbf{\Sigma} = \text{diag}(\sigma_1, \dots, \sigma_r).$$

The free parameters that explicitly appear above are $2r$ in total, and are given by the entries of the vector $\widehat{\mathbf{b}}$ and of the diagonal matrix $\mathbf{\Theta}$, i.e., the free parameters in the structured barycentric form (32) are $\{w_1, \dots, w_r\} \cup \{\theta_1, \dots, \theta_r\}$.

4 Computational methods

In this section, we discuss computational aspects for the construction of interpolating second-order models from data based on the different barycentric forms introduced in the previous section.

4.1 Linearized structured barycentric Loewner frameworks

The different barycentric forms presented in this paper are designed to interpolate, by construction, given transfer function data $\{(\lambda_i, h_i) \mid 1 \leq i \leq r\}$. However, in all three structured forms, free parameters remain. In the first-order case (Corollary 1), these can be used, for example, to interpolate additional transfer function data $\{(\mu_i, g_i) \mid 1 \leq i \leq r\}$, where it is assumed that the interpolation points of the two sets are distinct, i.e.,

$$\{\lambda_1, \dots, \lambda_r\} \cap \{\mu_1, \dots, \mu_r\} = \emptyset.$$

The resulting method can be seen as a barycentric transfer function version of the unstructured (first-order) Loewner framework [22].

Here, we aim to derive similar algorithms for the interpolation of additional transfer function data $\{(\mu_i, g_i) \mid 1 \leq i \leq r\}$ via the new structured barycentric forms (25), (27), and (32) by making use of the remaining free parameters. We can observe that (25) and (32) have $2r$ free parameters left, which potentially allow constructing of models that match the same number of interpolation conditions. However, the resulting systems of equations that need to be solved are nonlinear in the unknowns and, thus, need thorough investigations in

Algorithm 2: Linearized D -constrained second-order barycentric Loewner framework.

Input: Left and right interpolation data $\{(\lambda_i, h_i) \mid 1 \leq i \leq r\}$ and $\{(\mu_i, g_i) \mid 1 \leq i \leq r\}$, support points $\theta_1, \dots, \theta_r \in \mathbb{C}$.

Output: Second-order system matrices $\widehat{M}, \widehat{D}, \widehat{K}, \widehat{b}, \widehat{c}$.

1 Construct the r -dimensional divided differences matrix

$$\mathbf{L}_D = \begin{bmatrix} \frac{h_1 - \mu_1 g_1 \lambda_1^{-1}}{(\mu_1 - \lambda_1)(\mu_1 - \theta_1)} & \cdots & \frac{h_r - \mu_1 g_1 \lambda_r^{-1}}{(\mu_1 - \lambda_r)(\mu_1 - \theta_r)} \\ \vdots & \ddots & \vdots \\ \frac{h_1 - \mu_r g_r \lambda_1^{-1}}{(\mu_r - \lambda_1)(\mu_r - \theta_1)} & \cdots & \frac{h_r - \mu_r g_r \lambda_r^{-1}}{(\mu_r - \lambda_r)(\mu_r - \theta_r)} \end{bmatrix}.$$

2 Solve the linear system of equations $\mathbf{L}_D \mathbf{w} = \mathbf{g}$, for the unknown weights

$$\mathbf{w} = [w_1 \ \dots \ w_r]^\top \text{ and the given data } \mathbf{g} = [g_1 \ \dots \ g_r]^\top.$$

3 Construct the second-order system matrices

$$\widehat{M} = \mathbf{I}_r, \quad \widehat{D} = \widehat{b} \widehat{\mathbf{f}}^\top - \mathbf{\Lambda} - \mathbf{\Theta}, \quad \widehat{K} = \mathbf{\Theta} \mathbf{\Lambda}, \quad \widehat{b} = \mathbf{w}, \quad \widehat{c} = [h_1 \ \dots \ h_r]^\top,$$

$$\text{with } \widehat{\mathbf{f}}^\top = [\lambda_1^{-1} \ \dots \ \lambda_r^{-1}], \quad \mathbf{\Lambda} = \text{diag}(\lambda_1, \dots, \lambda_r) \text{ and } \mathbf{\Theta} = \text{diag}(\theta_1, \dots, \theta_r).$$

terms of solvability. For simplicity of exposition, we consider in this work only linearized versions of the equations by choosing “suitable” σ_i ’s in (25) and θ_i ’s in (32) a priori, leading to small linear systems to solve to satisfy additional r interpolation conditions. A discussion of heuristic choices for these support points is given in the upcoming Section 4.3.

The resulting methods based on the barycentric forms (25) and (32) are given in Algorithms 1 and 2. Both algorithms follow a similar structure. In Step 1 of Algorithms 1 and 2, the given interpolation data and support points are used to set up divided differences matrices. The realizations of these matrices are determined by the underlying barycentric forms (25) and (32).

For example, consider the barycentric form in (25). The goal is to find the weights $\mathbf{w} = [w_1 \ \dots \ w_r]^\top$ in this barycentric form (25) such that the additional interpolation conditions (35) for $\{(\mu_i, g_i) \mid 1 \leq i \leq r\}$ are satisfied. By inserting the form (25) into the interpolation conditions (35) and by multiplying both sides with the denominator of the barycentric form, we obtain the new relation

$$\sum_{i=1}^r \frac{h_i w_i}{(\mu_j - \lambda_i)(\mu_j - \sigma_i)} = g_j + \sum_{i=1}^r \frac{g_j w_i}{(\mu_j - \lambda_i)(\mu_j - \sigma_i)},$$

for $j = 1, \dots, r$. Bringing the terms with the unknowns w_1, \dots, w_r to the left-hand side yields the relation

$$\sum_{i=1}^r \frac{(h_i - g_j) w_i}{(\mu_j - \lambda_i)(\mu_j - \sigma_i)} = g_j, \quad (34)$$

for $j = 1, \dots, r$. Rearranging all equations of the form (34) such that the unknowns can be written as the vector $\mathbf{w} = [w_1 \ \dots \ w_r]^\top$ results in the linear system of equations

$$\mathbf{L}_K \mathbf{w} = \mathbf{g},$$

Algorithm 3: Second-order barycentric Loewner framework with zero damping.

Input: Left and right interpolation data $\{(\lambda_i, h_i) \mid 1 \leq i \leq r\}$ and $\{(\mu_i, g_i) \mid 1 \leq i \leq r\}$.

Output: Second-order system matrices $\widehat{\mathbf{M}}, \widehat{\mathbf{D}}, \widehat{\mathbf{K}}, \widehat{\mathbf{b}}, \widehat{\mathbf{c}}$.

1 Construct the r -dimensional divided difference matrix

$$\mathbf{L}_{\text{KD0}} = \begin{bmatrix} \frac{h_1 - g_1}{\mu_1^2 - \lambda_1^2} & \cdots & \frac{h_r - g_1}{\mu_1^2 - \lambda_r^2} \\ \vdots & \ddots & \vdots \\ \frac{h_1 - g_r}{\mu_r^2 - \lambda_1^2} & \cdots & \frac{h_r - g_r}{\mu_r^2 - \lambda_r^2} \end{bmatrix}.$$

2 Solve the linear system of equations $\mathbf{L}_{\text{KD0}}\mathbf{w} = \mathbf{g}$, for the unknown weights

$$\mathbf{w} = [w_1 \ \dots \ w_r]^\top \text{ and the given data } \mathbf{g} = [g_1 \ \dots \ g_r]^\top.$$

3 Construct the second-order system matrices

$$\widehat{\mathbf{M}} = \mathbf{I}_r, \quad \widehat{\mathbf{D}} = 0, \quad \widehat{\mathbf{K}} = \widehat{\mathbf{b}}\mathbf{1}_r^\top - \mathbf{\Lambda}^2, \quad \widehat{\mathbf{b}} = \mathbf{w}, \quad \widehat{\mathbf{c}} = [h_1 \ \dots \ h_r]^\top,$$

$$\text{with } \mathbf{\Lambda} = \text{diag}(\lambda_1, \dots, \lambda_r).$$

with the data vector $\mathbf{g} = [g_1 \ \dots \ g_r]^\top$ and the matrix of divided differences

$$\mathbf{L}_K = \begin{bmatrix} \frac{h_1 - g_1}{(\mu_1 - \lambda_1)(\mu_1 - \sigma_1)} & \cdots & \frac{h_r - g_1}{(\mu_1 - \lambda_r)(\mu_1 - \sigma_r)} \\ \vdots & \ddots & \vdots \\ \frac{h_1 - g_r}{(\mu_r - \lambda_1)(\mu_r - \sigma_1)} & \cdots & \frac{h_r - g_r}{(\mu_r - \lambda_r)(\mu_r - \sigma_r)} \end{bmatrix}.$$

This system of linear equations is then solved in Step 2 of [Algorithm 1](#). A similar derivation using [\(32\)](#) leads to the divided differences matrix in Step 1 of [Algorithm 2](#) and the solve of an analogous linear system of equations in Step 2 of [Algorithm 2](#). Under the assumption that the number of given data points r is less than the minimal system dimension and suitable choices of support points $\{\sigma_i\}$ and $\{\theta_i\}$ such that [Assumptions \(A1.2\)](#), [\(A2.1\)](#) and [\(A2.2\)](#) are satisfied for all interpolation points $\lambda_1, \dots, \lambda_r, \mu_1, \dots, \mu_r$, these linear systems of equations have unique solutions.

In Step 3 of [Algorithms 1](#) and [2](#), the second-order systems are constructed following the theory of [Theorems 1](#) and [2](#). In both cases, the transfer functions of the constructed systems satisfy the $2r$ imposed interpolation conditions

$$\widehat{H}(\lambda_1) = h_1, \quad \dots, \quad \widehat{H}(\lambda_r) = h_r, \quad \widehat{H}(\mu_1) = g_1, \quad \dots, \quad \widehat{H}(\mu_r) = g_r. \quad (35)$$

[Algorithm 3](#) shows the barycentric Loewner framework for the case of zero damping matrices based on [Corollary 2](#). While the main computational steps are following the same ideas as in [Algorithms 1](#) and [2](#), the difference to these methods is the lack of the set of support points $\{\sigma_i\}_{i=1, \dots, r}$ and $\{\theta_i\}_{i=1, \dots, r}$, which results from enforcing the $\widehat{\mathbf{D}} = 0$ damping model. The corresponding barycentric form [\(27\)](#) has r remaining free parameters that exactly allow the construction of an interpolating second-order system satisfying [\(35\)](#).

4.2 Construction of systems with real-valued matrices

A property desired in many applications for learned systems is the realization by means of real-valued matrices. This often allows the reinterpretation of the learned quantities and

the use of classical tools, established for real systems resulting, for example, from finite element discretizations. The key feature of second-order systems (1) with real matrices that needs to be exploited for the construction is that data at complex conjugate frequency points are also complex conjugate:

$$H(\bar{s}) = \mathbf{c}^\top (\bar{s}^2 \mathbf{M} + \bar{s} \mathbf{D} + \mathbf{K})^{-1} \mathbf{b} = \overline{\mathbf{c}^\top (s^2 \mathbf{M} + s \mathbf{D} + \mathbf{K})^{-1} \mathbf{b}} = \overline{H(s)}.$$

As in the classical Loewner framework, we assume the given data $\{(\lambda_i, h_i) \mid 1 \leq i \leq r\}$ and $\{(\mu_i, g_i) \mid 1 \leq i \leq r\}$ to be closed under conjugation in the respective sets. Additionally, for Algorithms 1 and 2, we need to assume that the support points $\{\sigma_i\}_{i=1,\dots,r}$ and $\{\theta_i\}_{i=1,\dots,r}$ are also closed under conjugation and that if λ_i, λ_{i+1} are complex conjugate, then so are σ_i, σ_{i+1} or θ_i, θ_{i+1} , respectively. Let the interpolation data and parameters be ordered such that complex conjugate are sorted together, e.g., for the interpolation points in $\{(\lambda_i, h_i) \mid 1 \leq i \leq r\}$, we have that

$$\lambda_1, \lambda_2 = \bar{\lambda}_1, \lambda_3, \lambda_4 = \bar{\lambda}_3, \dots$$

Given the matrices $\widehat{\mathbf{M}}, \widehat{\mathbf{D}}, \widehat{\mathbf{K}}, \widehat{\mathbf{b}}, \widehat{\mathbf{c}}$ computed by any of the Algorithms 1 to 3, a real-valued realization of the described system is given by

$$\overline{P}^\top \widehat{\mathbf{M}} \overline{P}, \overline{P}^\top \widehat{\mathbf{D}} \overline{P}, \overline{P}^\top \widehat{\mathbf{K}} \overline{P}, \overline{P}^\top \widehat{\mathbf{b}}, \widehat{\mathbf{c}} \overline{P},$$

where the transformation matrix P is block diagonal with

$$P = \text{diag}(J_1, J_2, \dots, J_\ell) \in \mathbb{C}^{r \times r},$$

and the block matrices are chosen according to the given interpolation data by

$$J_k = \begin{cases} \frac{1}{\sqrt{2}} \begin{bmatrix} 1 & -i \\ 1 & i \end{bmatrix} & \text{for complex conjugate interpolation points,} \\ 1 & \text{for real interpolation points.} \end{cases}$$

Remark 2. A special situation occurs in the case of Algorithm 3 for the construction of models with zero damping matrix. As discussed at the end of Section 3.2.2, the collection of data on the imaginary axis $i\mathbb{R}$ in complex conjugate pairs violates Assumption (A2.1). This is consistent with the observation that the corresponding transfer function yields identical values for complex conjugate points on the imaginary axis, i.e., for any $\mathbf{M}, \mathbf{K} \in \mathbb{C}^{n \times n}$, $\mathbf{D} = 0$ and $\mathbf{b}, \mathbf{c} \in \mathbb{C}^n$, it holds that

$$H(s) = \mathbf{c}^\top (s^2 \mathbf{M} + \mathbf{K})^{-1} \mathbf{b} = H(\bar{s}),$$

for all $s = i\omega \in i\mathbb{R}$. As a result, the collection of data from complex conjugate points on the imaginary axis yields no additional information due to the specific system structure and leads to singular linear systems in Step 2 of Algorithm 3. A side effect is that systems with zero damping and real matrices produce only real data on the imaginary axis such that no additional enforcement of real valued matrices is necessary.

4.3 Heuristics for choosing the support points

To discuss suitable choices for the support points $\sigma_1, \dots, \sigma_r$ and $\theta_1, \dots, \theta_r$, we consider their influence on the transfer functions (25) and (32). First, consider the case of the

barycentric form (25) resulting from the constrained stiffness matrix. Assume for the moment that $\sigma_1, \dots, \sigma_r$ are all distinct. Then, for the transfer function (25), it holds that

$$\widehat{H}(\sigma_i) = \frac{h_i w_i}{w_i} = h_i, \quad \text{for all } 1 \leq i \leq r,$$

i.e., the transfer function assumes the same values at the support points as at the interpolation points. Since the typical case will be $H(\lambda_i) \neq H(\sigma_i)$, this introduces approximation errors at the chosen support points. In the case that some of the support points are chosen to be identical, i.e., $\sigma_i = \sigma_{i_1} = \dots = \sigma_{i_\ell}$ for some indices i_1, \dots, i_ℓ , one can observe that

$$\widehat{H}(\sigma_i) = \frac{\sum_{k=1}^{\ell} h_{i_k} w_{i_k} (\sigma_i - \lambda_{i_k})}{\sum_{k=1}^{\ell} w_{i_k} (\sigma_i - \lambda_{i_k})}, \quad \text{for all } 1 \leq i \leq r, \quad (36)$$

holds. Similar to the case of distinct support points, approximation errors at σ_i are introduced. However, choosing many support points to be identical, allows to cluster the introduced errors away from frequency ranges of interest.

In a similar way, one can observe for the barycentric form (32) resulting from the constrained damping matrix that in the case of distinct support points $\theta_1, \dots, \theta_r$, it holds

$$\widehat{H}(\theta_i) = \frac{h_i w_i}{w_i \theta_i \lambda_i^{-1}} = \frac{h_i \lambda_i}{\theta_i}, \quad \text{for all } 1 \leq i \leq r.$$

As before, typically $H(\theta_i) \neq \frac{h_i \lambda_i}{\theta_i}$ will hold, indicating approximation errors introduced at the chosen support points. In the case that some of the support points are identical, i.e., $\theta_i = \theta_{i_1} = \dots = \theta_{i_\ell}$ for some indices i_1, \dots, i_ℓ , it holds that

$$\widehat{H}(\theta_i) = \frac{\sum_{k=1}^{\ell} h_{i_k} w_{i_k} (\theta_i - \lambda_{i_k})}{\sum_{k=1}^{\ell} \theta_i w_{i_k} \lambda_{i_k}^{-1} (\theta_i - \lambda_{i_k})}, \quad \text{for all } 1 \leq i \leq r. \quad (37)$$

To summarize, Equations (36) and (37) show that poorly chosen support points introduce undesired approximation errors. The points $\sigma_1, \dots, \sigma_r$ and $\theta_1, \dots, \theta_r$ do not need to be distinct (in contrast to the interpolation points; cf. Assumption (A1.2)), and the undesired approximation errors are enforced at the support points themselves. The second observation motivates to choose $\sigma_1, \dots, \sigma_r$ and $\theta_1, \dots, \theta_r$ outside the considered frequency region of interest, i.e.,

$$\sigma_k, \theta_k \notin \text{conv}_{\mathbb{R}}\{\lambda_1, \dots, \lambda_r, \mu_1, \dots, \mu_r\},$$

for $k = 1, \dots, r$ and where

$$\text{conv}_{\mathbb{R}}\{a_1, \dots, a_\ell\} := \left\{ z \in \mathbb{C} \mid z = \sum_{k=1}^{\ell} \beta_k a_k, \sum_{k=1}^{\ell} \beta_k = 1, \beta_1 \geq 0, \dots, \beta_\ell \geq 0 \right\}$$

denotes the convex hull of elements in \mathbb{C} over \mathbb{R} . This can be achieved, for example, by taking large shifts or multiples of the given interpolation points for the support points.

Next, we revisit the construction of the final second-order system matrices in Algorithms 1 and 2 and the influence of the support points on the properties of these matrices.

In both algorithms, the damping matrices take into account the negatives of the interpolation points $\lambda_1, \dots, \lambda_r$, which are subtracted by the chosen support points $\sigma_1, \dots, \sigma_r$ or $\theta_1, \dots, \theta_r$. Eigenvalues with positive real parts in the damping matrix can be interpreted as dissipation of energy from the system. To achieve this, a reasonable choice for $\sigma_1, \dots, \sigma_r$ and $\theta_1, \dots, \theta_r$ is to have negative real parts, which pushes the eigenvalues of the resulting damping matrix toward the right open half-plane. Especially, it is possible to construct real, symmetric positive definite damping matrices via [Algorithm 1](#) in the case that the interpolation data has been obtained on the imaginary axis by choosing the support points $\sigma_1, \dots, \sigma_r$ to yield

$$\operatorname{Re}(\sigma_i) < 0 \quad \text{and} \quad \operatorname{Im}(\sigma_i) = -\operatorname{Im}(\lambda_i), \quad \text{for all } i = 1, \dots, r. \quad (38)$$

On the other hand, we observe that the stiffness matrices in [Algorithms 1](#) and [2](#) involve the multiplication of the interpolation points $\lambda_1, \dots, \lambda_r$ with the support points $\sigma_1, \dots, \sigma_r$ and $\theta_1, \dots, \theta_r$. Aiming for stiffness matrices that have eigenvalues with positive real parts, which together with eigenvalues with positive real parts in the damping matrix drives the system towards asymptotic stability, the support points $\sigma_1, \dots, \sigma_r$ and $\theta_1, \dots, \theta_r$ should be chosen to have imaginary parts in the opposite half-plane of the imaginary parts of $\lambda_1, \dots, \lambda_r$, e.g., if the interpolation points are chosen over the positive imaginary axis, then $\sigma_1, \dots, \sigma_r$ and $\theta_1, \dots, \theta_r$ should have negative imaginary parts. In the case of [Algorithm 2](#) and the interpolation points $\lambda_1, \dots, \lambda_r$ to be on the imaginary axis, the support points $\theta_1, \dots, \theta_r$ can be chosen such that $\widehat{\mathbf{K}}$ can be realized as a real-valued, symmetric positive definite matrix by

$$\operatorname{Im}(\theta_i) = -(\operatorname{Im}(\lambda_i) + c_i), \quad \text{for all } i = 1, \dots, r,$$

where $c_i \in \mathbb{R}$ are real constants with the same sign as the imaginary part of λ_i such that $c_i \operatorname{Im}(\lambda_i) > 0$ holds.

5 Numerical experiments

In this section, we verify the proposed algorithms and barycentric forms numerically in different examples. The experiments reported here have been executed on a machine equipped with an AMD Ryzen 5 5500U processor running at 2.10 GHz and with 16 GB total main memory. The computer runs on Windows 10 Home version 21H2 (build 19044.2251) and, for all reported experiments, we use MATLAB 9.9.0.1592791 (R2020b). Source codes, data and numerical results are available at [\[43\]](#).

5.1 Computational setup

As setup of the subsequent comparative study, we consider the following data driven, interpolation-based methods:

soBaryLoewK the linearized K -constrained second-order barycentric Loewner framework from [Algorithm 1](#),

soBaryLoewD the linearized D -constrained second-order barycentric Loewner framework from [Algorithm 2](#),

soBaryLoewKD0 the second-order barycentric Loewner framework with zero damping matrix from [Algorithm 3](#),

Table 1: Dimensions and numbers of data samples for numerical examples. The amount of matched interpolation conditions for all constructed models is $2r$, due to the partition into left and right data. The column “c.c.d” denotes the use of complex conjugate interpolation points and data.

	full order	r	c.c.d.
Butterfly gyroscope	17 361	14	true
Artificial fishtail	779 232	6	true
Flexible aircraft	—	52	true
Bone model	986 703	19	false
Hysteretic plate	201 900	52	false

soLoewRayleigh the second-order (matrix) Loewner framework for Rayleigh-damped systems from [30],

BaryLoew the classical first-order barycentric Loewner framework based on the results in Corollary 1; see also [2].

All models are constructed such that the transfer functions satisfy the same interpolation conditions.

As interpolation points, we have chosen the local minima and maxima of the given data samples on the positive part of the imaginary axis using the MATLAB functions `islocalmin` and `islocalmax` supplemented by the limits of the considered frequency intervals of interest $[i\omega_{\min}, i\omega_{\max}]$ and, if necessary, some additional intermediate points. The interpolation points are then split into the left and right sets by alternating the ascending order of the positive imaginary parts, i.e.,

$$\text{Im}(\lambda_1) < \text{Im}(\mu_1) < \text{Im}(\lambda_2) < \text{Im}(\mu_2) < \dots < \text{Im}(\lambda_r) < \text{Im}(\mu_r).$$

For `soBaryLoewK` and `soBaryLoewD`, the support points are chosen according to the discussion in Section 4.3, more specifically as in (38). The individual choices are outlined in the description of the examples below. The Rayleigh damping parameters for `soLoewRayleigh` are either known from the original model or inferred in an optimal way. This means that we do not consider the optimization process of these additional parameters here.

For the comparison of the different methods, we consider the transfer function magnitude, given as the absolute value $|H(i\omega_k)|$, in the discrete frequency points $i\omega_k$ given in the data sets, and the corresponding pointwise relative errors via

$$\epsilon_{\text{rel}}(\omega_k) := \frac{|H(i\omega_k) - \widehat{H}(i\omega_k)|}{|H(i\omega_k)|}.$$

An overview providing the dimensions of the original full-order systems, the dimensions of the learned (reduced-order) models and if complex conjugate data has been used in the computations for the construction of real-valued system matrices can be found in Table 1. The rows of the table are split into the examples with and without damping matrix.

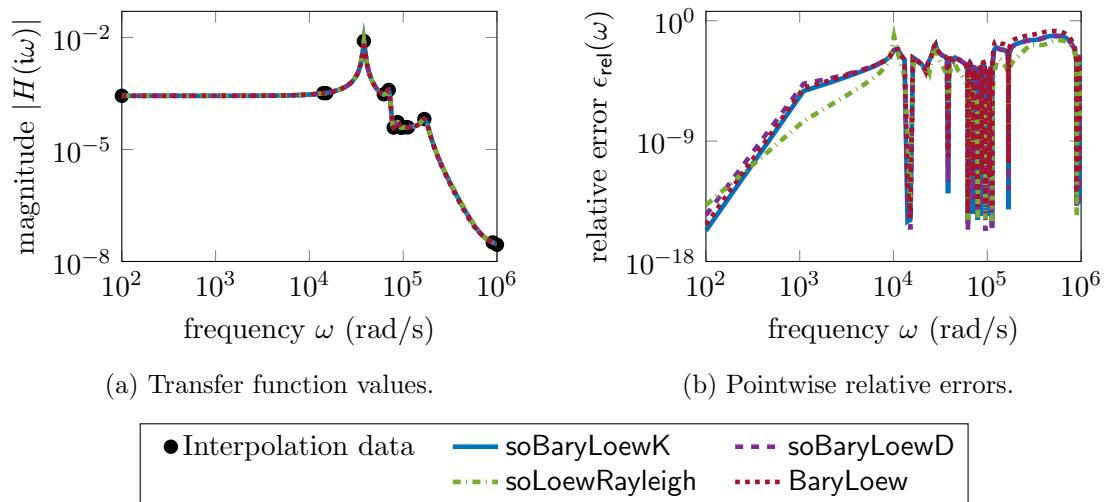


Figure 1: Butterfly gyroscope example: All methods recover reduced-order models with similar accuracy using the same amount of given interpolation data. The model learned by `soLoewRayleigh` performs slightly better for frequencies between 500 and 5 000 rad/s.

5.2 Examples with non-zero damping matrix

We first consider the case of models with energy dissipation, which need the presence of a damping matrix \hat{D} . Three examples are considered to test the proposed methods. The butterfly gyroscope models the behavior of a micro-mechanical vibrating gyroscope structure for the use in inertia-based navigation systems [10, 26]. The artificial fishtail models the deformation of a silicon structure in the shape of a fishtail used in the construction of underwater vehicles with fish-like locomotion [38, 39]. Lastly, we have sampled data from a high-fidelity simulation of a flexible aircraft model used in civil aeronautics to optimize lightweight structures [31, 32]. The dimensions of the sampled models and the dimension of the constructed second-order models are shown in Table 1. Note that we consider here SISO versions of these examples, which are originally single-input/multi-output.

The results computed by the different methods are shown in Figures 1 to 3, where we have set the support points as

$$\sigma_1 = \dots = \sigma_r = \theta_1 = \dots = \theta_r = -(5 + 10^{-3}i) \cdot \omega_{\max}$$

for the butterfly gyroscope and flexible aircraft, and

$$\sigma_1 = \dots = \sigma_r = \theta_1 = \dots = \theta_r = -(5 + 10^{-5}i) \cdot \omega_{\max}$$

in the case of the fishtail example, where $\omega_{\max} \in \mathbb{R}$ is the upper limit of the considered frequency interval. The figures show the transfer function magnitudes of the constructed models with the used interpolation data and the pointwise relative errors computed with respect to all given data samples. In the case of the butterfly and fishtail examples, these are 1 000 samples in the frequency range of interest and 421 samples for the flexible aircraft example. For all three examples, the considered methods perform similarly well in terms of the pointwise relative errors shown in Figures 1 to 3. However, we can note that the learned models assume different spectral properties. In the case of the butterfly gyroscope, the proposed methods `soBaryLoewK` and `soBaryLoewD` produce asymptotically stable reduced-order models due to the choice of support points, in contrast to the classical

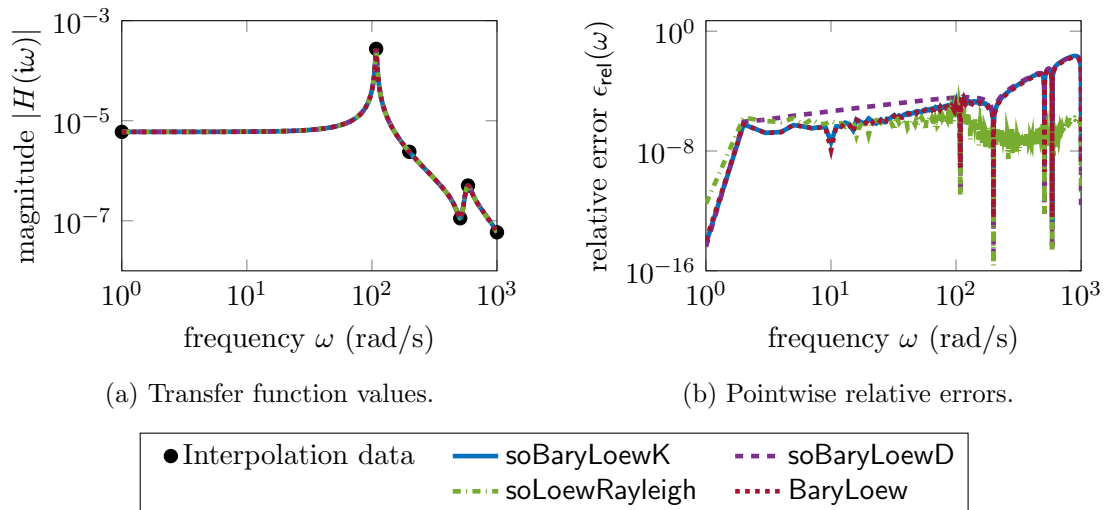


Figure 2: Artificial fishtail example: All methods provide a similar approximation accuracy. The model inferred by `soBaryLoewD` performs insignificantly worse for frequencies between 1 and 100 rad/s, while the model from `soLoewRayleigh` keeps the accuracy level also for higher frequencies.

`BaryLoew`, which has one unstable pole. The Rayleigh-damped approach `soLoewRayleigh` gives one unstable and one infinite eigenvalue, where the infinite one likely results from the finite arithmetic in the eigenvalue computations and the highly ill-conditioned learned system matrices. For the fishtail example, all computed reduced-order models are stable and for the aircraft example, no reduced-order model is stable. In particular, `soBaryLoewD`, `soLoewRayleigh` and `BaryLoew` have three pairs of unstable complex conjugate eigenvalues, while `soBaryLoewK` has only two pairs.

5.3 Examples with zero damping matrix

Now, we consider two examples with zero damping matrix, in order to test `soBaryLoewKD0`. First, we have the bone model as a conservative system, which is used to simulate the porous bone micro-architecture in studies of bone tissue under different loads [25, 41]. As a second example, we consider the model of a vibrating plate that is equipped with tuned vibration absorbers, which lead to hysteretic structural damping [4, 5]. The results of the different methods can be seen in Figures 4 and 5. In both examples, the second-order methods `soBaryLoewKD0` and `soLoewRayleigh` perform better in terms of the pointwise relative errors than the classical `BaryLoew`. This comes from the additional preservation of the damping model in these methods. In particular, we can observe that in the absence of any type of energy dissipation, the two methods that preserve the zero damping structure outperform the classical Loewner framework by several orders of magnitude.

Additionally, we note that the curves of `soBaryLoewKD0` and `soLoewRayleigh` are in fact identical in both examples. This is a numerical verification that the barycentric form in Corollary 2 describes exactly the same system that is recovered by `soLoewRayleigh` with zero Rayleigh damping parameters, i.e., both methods construct different realizations of exactly the same interpolatory second-order systems.

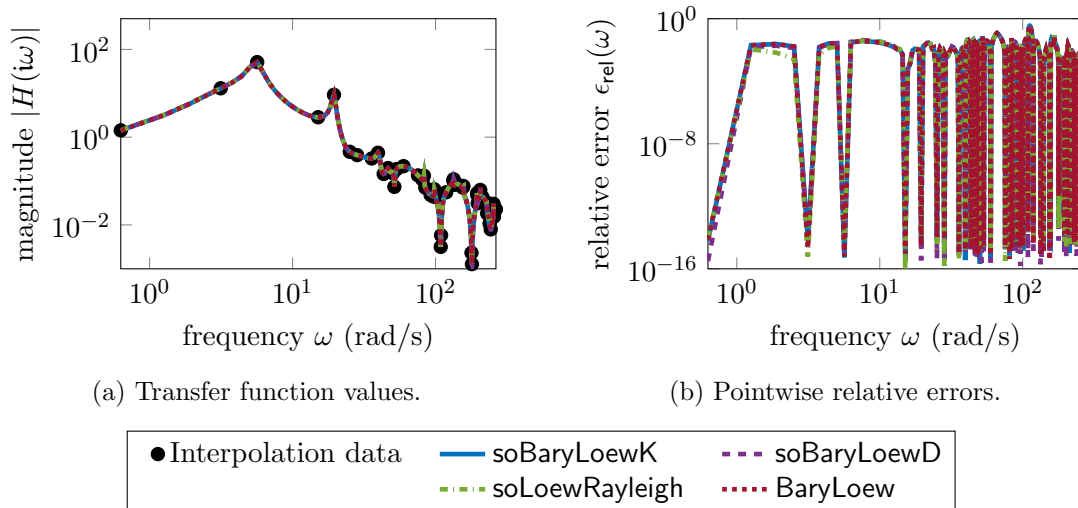


Figure 3: Flexible aircraft example: All methods construct reduced-order models that recover the given data set with sufficient accuracy. For higher frequencies, more interpolation data is used due to the presence of many local maxima and minima.

6 Conclusions

We have developed new structured barycentric forms for the transfer functions of second-order systems for data-driven, interpolatory reduced-order modeling. Based on these barycentric forms, we have proposed three Loewner-like algorithms for the construction of second-order systems from data. Numerical experiments compared these new methods to the classical, unstructured Loewner approach as well as to another Loewner-like method for the construction of second-order systems from frequency domain data. In all examples, the new structured approaches were able to provide a similar, and in some cases significantly better, approximation accuracy as the established methods from the literature some of which do not obey to preserve the structure. Since the proposed algorithms rely on some fixed parameter choices to simplify computations, we expect that including these additional “support points” as parameters would significantly increase the approximation capabilities of methods based on the presented structured barycentric forms. However, we leave these considerations for future work. Additionally, we have observed that these support points can be used to alter the properties of the constructed system matrices, allowing, for example, the construction of asymptotically stable second-order systems.

At the heart of this work are the new structured barycentric forms that allow for a large bandwidth of new algorithms for learning structured models from frequency domain data. For the clarity of the presentation, we restricted the analysis in this work to a purely interpolatory framework. However, the use of the free parameters in the barycentric forms for least-squares fitting will allow the derivation of methods like vector fitting [17] and AAA [24] for second-order systems. In particular, the presence of more parameters than in the unstructured, first-order system case gives rise to a lot more variety in resulting algorithms. We will consider these ideas in future work.

Acknowledgments

The work of Gugercin is based upon work supported by the National Science Foundation under Grant No. AMPS-1923221.

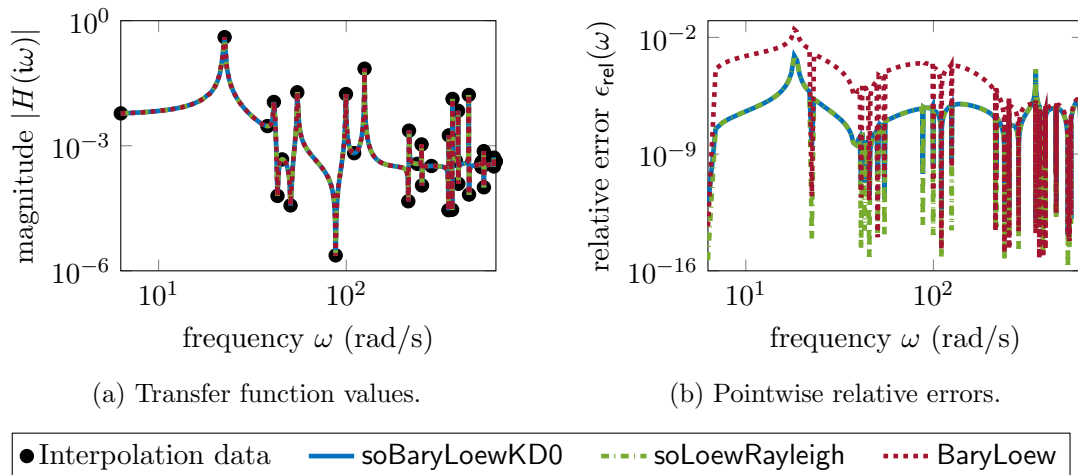


Figure 4: Bone model example: For lower frequencies, the second-order methods produce models with at least one order of magnitude smaller relative errors than the classical Loewner framework. The curves of soBaryLoewKD0 and soLoewRayleigh are identical up to numerical round-off errors.

References

- [1] R. Abraham and J. E. Marsden. *Foundations of Mechanics*. Addison-Wesley Publishing Company, Inc., Redwood City, second edition, 1987. URL: <https://resolver.caltech.edu/CaltechB00K:1987.001>.
- [2] A. C. Antoulas and B. D. O. Anderson. On the scalar rational interpolation problem. *IMA J. Math. Control Inf.*, 3(2–3):61–8, 1986. doi:10.1093/imamci/3.2-3.61.
- [3] A. C. Antoulas, C. A. Beattie, and S. Gugercin. *Interpolatory Methods for Model Reduction*. Computational Science & Engineering. SIAM, Philadelphia, PA, 2020. doi:10.1137/1.9781611976083.
- [4] Q. Aumann and S. W. R. Werner. Code, data and results for numerical experiments in “Structured model order reduction for vibro-acoustic problems using interpolation and balancing methods” (version 1.1), August 2022. doi:10.5281/zenodo.6806016.
- [5] Q. Aumann and S. W. R. Werner. Structured model order reduction for vibro-acoustic problems using interpolation and balancing methods. *J. Sound Vib.*, 543:117363, 2023. doi:10.1016/j.jsv.2022.117363.
- [6] C. A. Beattie and S. Gugercin. Interpolatory projection methods for structure-preserving model reduction. *Syst. Control Lett.*, 58(3):225–232, 2009. doi:10.1016/j.sysconle.2008.10.016.
- [7] C. A. Beattie and S. Gugercin. Realization-independent \mathcal{H}_2 -approximation. In *51st IEEE Conference on Decision and Control (CDC)*, pages 4953–4958, 2012. doi:10.1109/CDC.2012.6426344.
- [8] M. Berljafa and S. Güttel. The RKFIT algorithm for nonlinear rational approximation. *SIAM J. Sci. Comput.*, 39(5):A2049–A2071, 2017. doi:10.1137/15M1025426.
- [9] J.-P. Berrut and L. N. Trefethen. Barycentric Lagrange interpolation. *SIAM Rev.*, 46(3):501–517, 2004. doi:10.1137/S0036144502417715.

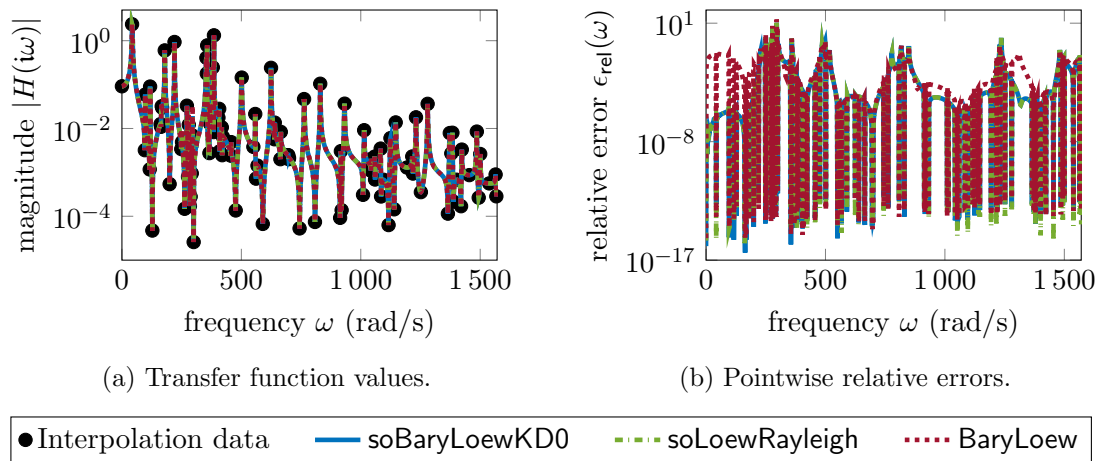


Figure 5: Hysteretic plate example: For up to 50 rad/s, the second-order methods soBaryLoewKD0 and soLoewRayleigh produce relative errors that are at least four orders of magnitude smaller than the classical BaryLoew. The curves of soBaryLoewKD0 and soLoewRayleigh are identical up to numerical round-off.

- [10] D. Billger. The butterfly gyro. In P. Benner, V. Mehrmann, and D. C. Sorensen, editors, *Dimension Reduction of Large-Scale Systems*, volume 45 of *Lect. Notes Comput. Sci. Eng.*, pages 349–352. Springer, Berlin, Heidelberg, 2005. doi:10.1007/3-540-27909-1_18.
- [11] F. Blaabjerg. *Control of Power Electronic Converters and Systems: Volume 2*. Academic Press, London, 2018. doi:10.1016/C2017-0-04756-0.
- [12] S. L. Brunton and J. N. Kutz. *Data-Driven Science and Engineering: Machine Learning, Dynamical Systems, and Control*. Cambridge University Press, Cambridge, 2019. doi:10.1017/9781108380690.
- [13] J. T. Chen and D. W. You. Hysteretic damping revisited. *Adv. Eng. Softw.*, 28(3):165–171, 1997. doi:10.1016/S0965-9978(96)00052-X.
- [14] Z. Drmač, S. Gugercin, and C. Beattie. Quadrature-based vector fitting for discretized \mathcal{H}_2 approximation. *SIAM J. Sci. Comput.*, 37(2):A625–A652, 2015. doi:10.1137/140961511.
- [15] Y. Filanova, I. Pontes Duff, P. Goyal, and P. Benner. An operator inference oriented approach for mechanical systems. e-print 2210.07710, arXiv, 2022. Dynamical Systems (math.DS). doi:10.48550/arXiv.2210.07710.
- [16] G. H. Golub and C. F. Van Loan. *Matrix Computations*. Johns Hopkins Studies in the Mathematical Sciences. Johns Hopkins University Press, Baltimore, fourth edition, 2013.
- [17] B. Gustavsen and A. Semlyen. Rational approximation of frequency domain responses by vector fitting. *IEEE Trans. Power Del.*, 14(3):1052–1061, 1999. doi:10.1109/61.772353.
- [18] J.-N. Juang and R. S. Pappa. An eigensystem realization algorithm for modal parameter identification and model reduction. *J. Guid. Control Dyn.*, 8(5):620–627, 1985. doi:10.2514/3.20031.

- [19] B. Kramer and A. A. Gorodetsky. System identification via CUR-factored Hankel approximation. *SIAM J. Sci. Comput.*, 40(2):A848–A866, 2018. doi:10.1137/17M1137632.
- [20] S.-Y. Kung. A new identification and model reduction algorithm via singular value decomposition. In *Proceedings of the 12th Asilomar Conference on Circuits, Systems, and Computers, Pacific Grove, CA*, pages 705–714, 1978.
- [21] N. Lobontiu. *System Dynamics for Engineering Students: Concepts and Applications*. Academic Press, London, second edition, 2018. doi:10.1016/C2011-0-05346-2.
- [22] A. J. Mayo and A. C. Antoulas. A framework for the solution of the generalized realization problem. *Linear Algebra Appl.*, 425(2–3):634–662, 2007. Special issue in honor of P. A. Fuhrmann, Edited by A. C. Antoulas, U. Helmke, J. Rosenthal, V. Vinnikov, and E. Zerz. doi:10.1016/j.laa.2007.03.008.
- [23] K. R. Meyer and D. C. Offin. *Introduction to Hamiltonian Dynamical Systems and the N-Body Problem*, volume 90 of *Appl. Math. Sci.* Springer, Cham, 2017. doi:10.1007/978-3-319-53691-0.
- [24] Y. Nakatsukasa, O. Sète, and L. N. Trefethen. The AAA algorithm for rational approximation. *SIAM J. Sci. Comput.*, 40(3):A1494–A1522, 2018. doi:10.1137/16M1106122.
- [25] Oberwolfach Benchmark Collection. Bone model. hosted at MORwiki – Model Order Reduction Wiki, 2005. URL: http://modelreduction.org/index.php/Bone_Model.
- [26] Oberwolfach Benchmark Collection. Butterfly gyroscope. hosted at MORwiki – Model Order Reduction Wiki, 2005. URL: http://modelreduction.org/index.php/Butterfly_Gyroscope.
- [27] B. Peherstorfer. Sampling low-dimensional Markovian dynamics for preasymptotically recovering reduced models from data with operator inference. *SIAM J. Sci. Comput.*, 42(5):A3489–A3515, 2020. doi:10.1137/19M1292448.
- [28] B. Peherstorfer, S. Gugercin, and K. Willcox. Data-driven reduced model construction with time-domain Loewner models. *SIAM J. Sci. Comput.*, 39(5):A2152–A2178, 2017. doi:10.1137/16M1094750.
- [29] B. Peherstorfer and K. Willcox. Data-driven operator inference for nonintrusive projection-based model reduction. *Comput. Methods Appl. Mech. Eng.*, 306:196–215, 2016. doi:10.1016/j.cma.2016.03.025.
- [30] I. Pontes Duff, P. Goyal, and P. Benner. Data-driven identification of Rayleigh-damped second-order systems. In C. Beattie, P. Benner, M. Embree, S. Gugercin, and S. Lefteriu, editors, *Realization and Model Reduction of Dynamical Systems*, pages 255–272. Springer, Cham, 2022. doi:10.1007/978-3-030-95157-3_14.
- [31] C. Poussot-Vassal, D. Quero, and P. Vuillemin. Data-driven approximation of a high fidelity gust-oriented flexible aircraft dynamical model. *IFAC-Pap.*, 51(2):559–564, 2018. 9th Vienna International Conference on Mathematical Modelling MATHMOD 2018. doi:10.1016/j.ifacol.2018.03.094.

- [32] C. Poussot-Vassal, D. Quero, and P. Vuillemin. Flexible aircraft. hosted at MORwiki – Model Order Reduction Wiki, 2018. URL: http://modelreduction.org/index.php/Flexible_Aircraft.
- [33] E. Qian, B. Kramer, B. Peherstorfer, and K. Willcox. Lift & Learn: Physics-informed machine learning for large-scale nonlinear dynamical systems. *Phys. D: Nonlinear Phenom.*, 406:132401, 2020. doi:10.1016/j.physd.2020.132401.
- [34] J. Saak, D. Siebelts, and S. W. R. Werner. A comparison of second-order model order reduction methods for an artificial fishtail. *at-Automatisierungstechnik*, 67(8):648–667, 2019. doi:10.1515/auto-2019-0027.
- [35] P. J. Schmid. Dynamic mode decomposition of numerical and experimental data. *J. Fluid Mech.*, 656:5–28, 2010. doi:10.1017/S0022112010001217.
- [36] P. Schulze, B. Unger, C. Beattie, and S. Gugercin. Data-driven structured realization. *Linear Algebra Appl.*, 537:250–286, 2018. doi:10.1016/j.laa.2017.09.030.
- [37] H. Sharma and B. Kramer. Preserving Lagrangian structure in data-driven reduced-order modeling of large-scale dynamical systems. e-print 2203.06361, arXiv, 2022. Numerical Analysis (math.NA). doi:10.48550/arXiv.2203.06361.
- [38] D. Siebelts, A. Kater, and T. Meurer. Modeling and motion planning for an artificial fishtail. *IFAC-Pap.*, 51(2):319–324, 2018. 9th Vienna International Conference on Mathematical Modelling MATHMOD 2018. doi:10.1016/j.ifacol.2018.03.055.
- [39] D. Siebelts, A. Kater, T. Meurer, and J. Andrej. Matrices for an artificial fishtail. hosted at MORwiki – Model Order Reduction Wiki, 2019. doi:10.5281/zenodo.2558728.
- [40] J. H. Tu, C. W. Rowley, D. M. Luchtenburg, S. L. Brunton, and J. N. Kutz. On dynamic mode decomposition: Theory and applications. *J. Comput. Dyn.*, 1(2):391–421, 2014. doi:10.3934/jcd.2014.1.391.
- [41] B. Van Rietbergen, H. Weinans, R. Huiskes, and A. Odgaard. A new method to determine trabecular bone elastic properties and loading using micromechanical finite-element models. *J. Biomech.*, 28(1):69–81, 1995. doi:10.1016/0021-9290(95)80008-5.
- [42] S. W. R. Werner. *Structure-Preserving Model Reduction for Mechanical Systems*. Dissertation, Otto-von-Guericke-Universität, Magdeburg, Germany, 2021. doi:10.25673/38617.
- [43] S. W. R. Werner. Code, data and results for numerical experiments in “Structured barycentric forms for interpolation-based data-driven reduced modeling of second-order systems” (version 1.0), March 2023. doi:10.5281/zenodo.7358813.
- [44] S. W. R. Werner, I. V. Gosea, and S. Gugercin. Structured vector fitting framework for mechanical systems. *IFAC-Pap.*, 55(20):163–168, 2022. 10th Vienna International Conference on Mathematical Modelling MATHMOD 2022. doi:10.1016/j.ifacol.2022.09.089.